AEDC-TR-76-142

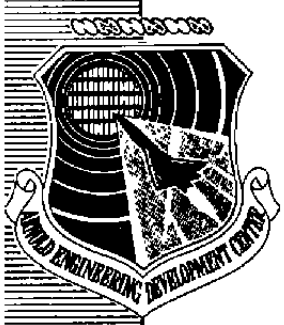

# EVALUATION OF THE AERODYNAMIC INTERFERENCE OF THE TUNNEL 4T CAPTIVE TRAJECTORY SYSTEM ON THE SEPARATION CHARACTERISTICS OF THE BLU-27 STORE


PROPULSION WIND TUNNEL FACILITY
ARNOLD ENGINEERING DEVELOPMENT CENTER
AIR FORCE SYSTEMS COMMAND
ARNOLD AIR FORCE STATION, TENNESSEE 37389



November 1976


Final Report for Period December 1975 — July 1976

Approved for public release, distribution unlimited


Prepared for

DIRECTORATE OF TECHNOLOGY (DY)
ARNOLD ENGINEERING DEVELOPMENT CENTER
ARNOLD AIR FORCE STATION, TENNESSEE 37389

## NOTICES

When U. S. Government drawings specifications, or other data are used for any purpose other than a definitely related Government procurement operation, the Government thereby incurs no responsibility nor any obligation whatsoever, and the fact that the Government may have formulated, furnished, or in any way supplied the said drawings, specifications, or other data, is not to be regarded by implication or otherwise, or in any manner licensing the holder or any other person or corporation, or conveying any rights or permission to manufacture, use, or sell any patented invention that may in any way be related thereto.

Qualified users may obtain copies of this report from the Defense Documentation Center.

References to named commercial products in this report are not to be considered in any sense as an endorsement of the product by the United States Air Force or the Government.

This report has been reviewed by the Information Office (OI) and is releasable to the National Technical Information Service (NTIS). At NTIS, it will be available to the general public, including foreign nations.

## APPROVAL STATEMENT

This technical report has been reviewed and is approved for publication.

FOR THE COMMANDER

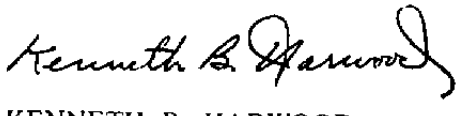

KENNETH B. HARWOOD
Major, CF
Research & Development
Division
Directorate of Technology

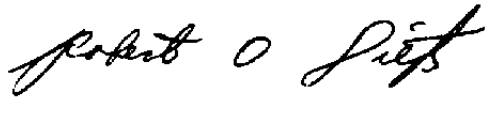

ROBERT O. DIETZ
Director of Technology

| REPORT DOCUMENTATION PAGE | | READ INSTRUCTIONS BEFORE COMPLETING FORM |
|---|---|---|
| 1 REPORT NUMBER<br>AEDC-TR-76-142 | 2 GOVT ACCESSION NO. | 3 RECIPIENT'S CATALOG NUMBER |
| 4 TITLE (and Subtitle) EVALUATION OF THE AERODYNAMIC INTERFERENCE OF THE TUNNEL 4T CAPTIVE TRAJECTORY SYSTEM ON THE SEPARATION CHARACTERISTICS OF THE BLU-27 STORE | | 5 TYPE OF REPORT & PERIOD COVERED<br>Final Report - Dec 1975 - July 1976<br>6 PERFORMING ORG REPORT NUMBER |
| 7 AUTHOR(s)<br>Wallace Luchuk and David W. Hill, Jr., ARO, Inc. | | 8 CONTRACT OR GRANT NUMBER(s) |
| 9 PERFORMING ORGANIZATION NAME AND ADDRESS<br>Arnold Engineering Development Center (DY)<br>Air Force Systems Command<br>Arnold Air Force Station, Tennessee 37389 | | 10 PROGRAM ELEMENT PROJECT, TASK AREA & WORK UNIT NUMBERS<br>Program Element 65807F |
| 11 CONTROLLING OFFICE NAME AND ADDRESS<br>Arnold Engineering Development Center(DYFS)<br>Air Force Systems Command<br>Arnold Air Force Station, Tennessee 37389 | | 12 REPORT DATE<br>November 1976<br>13 NUMBER OF PAGES<br>52 |
| 14 MONITORING AGENCY NAME & ADDRESS(if different from Controlling Office) | | 15 SECURITY CLASS (of this report)<br>UNCLASSIFIED<br>15a DECLASSIFICATION DOWNGRADING SCHEDULE<br>N/A |

16 DISTRIBUTION STATEMENT (of this Report)

Approved for public release; distribution unlimited.

17 DISTRIBUTION STATEMENT (of the abstract entered in Block 20, if different from Report)

18 SUPPLEMENTARY NOTES

Available in DDC

19 KEY WORDS (Continue on reverse side if necessary and identify by block number)

captive tests
trajectories
aerodynamic forces
interference
external stores
separation
transonic flow
wind tunnel tests

20 ABSTRACT (Continue on reverse side if necessary and identify by block number)

This report contains the results of an experimental program to evaluate the effect of the 4T Captive Trajectory System on the separation characteristics of "typical" stores. The models selected as being generally representative of external stores were the modified BLU-27B/B configuration with and without fins. The aircraft model selected for this test was the F-111. To assess the aerodynamic interference of the Captive Trajectory System on

DD FORM 1 JAN 73 1473 EDITION OF 1 NOV 65 IS OBSOLETE

20. ABSTRACT (Continued)

the store and its trajectory, four sting lengths were used to position the store model at varying distances from the support system. Data were obtained at Mach numbers of 0.4, 0.8, 0.9, 1.1, and 1.2. Captive trajectories simulating store separation from the aircraft model were obtained; forces on the store were measured while the store was moved vertically away from the carriage position; and force data on the store were obtained as it was yawed in a location as far removed as possible from the aircraft model. It was concluded that the Captive Trajectory System has little or no effect on the store loads and trajectory development.

AFSC
Arnold AFS Tenn

## PREFACE

The work reported herein was conducted by the Arnold Engineering Development Center (AEDC), Air Force Systems Command (AFSC), under Program Element 65807F. The results presented were obtained by ARO, Inc. (a subsidiary of Sverdrup & Parcel and Associates, Inc.), contract operator of AEDC, AFSC, Arnold Air Force Station, Tennessee. The information presented was obtained under ARO Project No. P32A-D1A. The authors of this report were Wallace Luchuk and David W. Hill, Jr., ARO, Inc. The manuscript (ARO Control No. ARO-PWT-TR-76-98) was submitted for publication on August 25, 1976.

## CONTENTS



## ILLUSTRATIONS

Figure

## TABLE

# 1.0 INTRODUCTION

The Captive Trajectory System (CTS) is a model support system for store separation testing capable of providing the store model with six degrees of freedom under the direction of a computer (Ref. 1). Relatively long stings are used to ensure that the support system does not contribute any adverse aerodynamic effects on the separation motion. However, the use of long stings has often resulted in curtailed trajectories. These curtailed trajectories result when the store models are pitched to high angles of attack (or yaw) while keeping the center of gravity of the stores relatively fixed in space. This type of motion requires an extreme, vertical or lateral movement of the aft end of the sting (and the pitch-yaw head of the CTS) and often one of the mechanical limits of movement would be reached (see Fig. 1).

During a design study for a new pitch-yaw-roll head for the CTS, a computer study was made using a potential flow program to calculate the interference flow field of the present CTS. The results of this computer study showed that the perturbation in Mach number (attributable to the CTS head) at a point about 12 in. in front of the apex of the conical head was one percent or less of the free-stream Mach number. A previous experimental study, in which the static pressure was measured along a tubular probe mounted in the CTS head to determine tunnel Mach number distributions, was re-evaluated with regard to support head interference. The probe static pressure distributions clearly revealed the perturbation of the CTS head on the flow field. The results of the static pressure probe measurements (converted to deviations from the free-stream Mach number) are presented in Fig. 2 along with the results of the computer study. Also presented in Fig. 2 is a sketch of the static pressure probe. The experimental results are in rough agreement with the calculated results, and the rapid diminution in interference with distance from the CTS head confirms the very small interference effect at about 12 in. These results prompted the consideration of the effect of a one-percent perturbation in Mach number

on the static aerodynamic coefficients of typical stores. The typical store is a rather slender low-drag body that may or may not have small low-aspect-ratio fins. In either case, these types of stores usually have lift coefficient slopes, $dC_L/d\alpha$, and pitching-moment coefficient slopes, $dC_m/d\alpha$, that do not change greatly as the Mach number is varied. The low sensitivities of typical stores to Mach number variations and the apparently low interference of the CTS head suggests that the interference effects on trajectory development might be insignificant--at least for a sting 12 or more inches in length.

This background information prompted the initiation of a test program to experimentally verify these inferences. A store model was positioned at varying distances from the bulk of the support system by using stings that varied only in length. Aerodynamic forces and trajectories of the store, for the varying sting lengths, are presented.

## 2.0 TEST APPARATUS

This test was conducted in the AEDC Aerodynamic Wind Tunnel (4T), a closed-loop, continuous flow, variable density tunnel in which the Mach number can be varied from 0.1 to 1.3. At all Mach numbers, the stagnation pressure can be varied from 300 to 3,700 psfa. The test section is 4 ft square and 12.5 ft long with perforated, variable porosity (0.5- to 10-percent open) walls. It is completely enclosed in a plenum chamber from which the air can be evacuated, allowing part of the tunnel airflow to be removed through the perforated walls of the test section. The tunnel has provisions for two model support systems: a main support system on which the aircraft model is attached and the CTS which supports the store model. The main support system allows the aircraft model to pitch, and the CTS provides the store model with six degrees of freedom of motion. The aircraft model is installed on the main support in an inverted position about 6 in. below

the tunnel centerline. The store model is then positioned close to any of the several carriage points on the aircraft model before the start of trajectory development.

A sketch of the wind tunnel test section with the installation of the F-111 aircraft model and the store model is shown in Fig. 3. A photograph of the test installation is presented in Fig. 4.

## 3.0 MODEL HARDWARE

The store model selected for testing was a 1/20-scale model of the BLU-27B/B configuration. This configuration was considered generally representative of most of the external stores carried by present-day aircraft. The basic BLU-27B/B shown in Fig. 5 was modified at the base to permit the installation of a support sting. A finless version of the modified BLU-27B/B was also selected to determine if the effects of support head interference were the same on aerodynamically unstable stores as on stable stores. A sketch of the finless BLU-27B/B store model is presented in Fig. 6.

One of the considerations for selecting the BLU-27B/B model was that it has a boattail afterbody. It is well known that sting or support system interference is manifested as changes in boattail surface and base pressure. Any support system interference effects would be more pronounced with the boattail afterbody and produce changes in the normal force and pitching moment (and/or side force and yawing moment). It was through these changes in the store aerodynamic forces that support interference effects were intended to be revealed. The physical properties of the store are given in Table 1.

The aircraft model selected from the several available was the 1/24-scale F-111 model (see Fig. 7). The F-111 model was selected for several reasons. First, it is supported by a dorsal blade or strut which provides vacant space to the rear of the model. This vacant space provides freedom of motion for the CTS and the trajectory development. In addition, the F-111 aircraft is a shoulder-wing type of aircraft and, as such, develops strong gradients in the local flow field in both the pitch and yaw planes. These flow fields could produce significant store motions in both planes. Thus, the effect of support system interference on separation could be assessed from the motion of the store in two planes. The leading-edge sweep angle of the F-111 wing was 26 deg for this test program.

The carriage location selected to be used was pylon position 6 (see Fig. 7). Pylon position 5 was considered a more desirable carriage location from the standpoint of the presence of stronger local flow fields; however, it was found that this carriage position could not be reached because of physical interference between the F-111 fuselage afterbody and the CTS head when the shorter stings were used. A sketch of the 1/24-scale position 6 pylon is presented in Fig. 8.

A sketch is presented in Fig. 9 of an unfinned BLU-27B/B installed on the variable length sting. The force balance which measured the store aerodynamic loads was fabricated with a 0.400-in.-diam sting which projected about 2 in. behind the store. The balance sting was attached to 0.750-in.-diam stings of varying lengths. The lengths are shown in Fig. 9 and are nominally called 3-, 5-, 7-, and 13-in. stings in subsequent discussions.

It should be noted that the store model was a 1/20-scale model of a real store and the aircraft model was a 1/24-scale model of the prototype. However, this difference in scales should not detract from the general conclusions of this test since differences in trajectories were of interest and not actual trajectories.

A base pressure tube was installed on each configuration to provide the most direct and sensitive indication of support system interference effects.

The sting lengths that were selected were intended to produce a variation in store forces and trajectories from which an "interference-free" sting length could be determined. The two shorter stings were, in fact, impractically short because with these shorter lengths the conical tip of the CTS was alongside the aircraft model afterbody and the yaw center of the CTS was only a short distance aft of the aircraft model fuselage base (FS 32.676 in Fig. 7). The shorter length stings were deliberately selected to produce significant interference effects.

## 4.0 TEST PROCEDURE

Three procedures were followed in this test program. The first resulted in the conventional "trajectory" development. The second was a "grid" procedure in which the model was moved vertically away from the carriage point in fixed increments while the aerodynamic forces were measured at each location. The third procedure consisted of moving the store model as far away from the aircraft model (vertically and forward) as the CTS would allow. At this location the store was yawed through an angle range while the aerodynamic forces were measured. This procedure was called the "free-stream" procedure.

In the trajectory procedure, the store was initially positioned in the carriage position. The trajectory was initiated, and the store was free to move under the influence of the application of ejector forces, inertia forces, and aerodynamic forces as determined by the six-degree-of-freedom equations of motion. The trajectory was developed in small non-real-time increments using the inertial properties of the full-scale store and the atmospheric density and the dynamic pressure of the full-scale aircraft and store at flight conditions. The second or

grid procedure was used to evaluate the CTS interference effects in close to the carriage location. At this location, the effects of the local flow field of the aircraft model are most pronounced, and differences in the forces on the store attributable to sting length would imply that the CTS had an effect on the flow field of the aircraft model. The third test procedure was carried out to evaluate the direct interference of the CTS on the aerodynamic characteristics of the store itself. By moving the store out of the flow field of the aircraft model, the effect of varying the sting length on the store aerodynamics could be determined.

All three test procedures were applied to both the finned and the unfinned stores at Mach numbers of 0.4, 0.8, 0.9, 1.1, and 1.2. The tunnel total pressure was fixed at 1,200 psfa at all Mach numbers.

In performing the trajectory development, an ejector force and moment which are characteristic of the full-scale hardware were applied to the store in the equations of motion to give the store an initial vertical velocity, $\dot{z}$, and an initial pitching velocity, $\dot{\theta}$. Since the store model and aircraft model for this test program were not representative of a real aircraft model and store (scale-wise), the ejector force and moment were arbitrary variables. It was desirable to select a representative ejector force and moment which would also be "typical" of real separation. However, it was more important that the trajectories proceed sufficiently in space so that reasonable comparisons between trajectories could be made. In other words, it was more important to have long trajectories than to have "real" trajectories.

Upon initiation of the trajectories at the higher Mach numbers (0.9 and above), it was found that the local flow field of the parent aircraft caused the stores to pitch nose-down. This nose-down pitching moment led to a premature termination of the trajectories, because the CTS was driven to its upper extremity: the back end of the sting must

move vertically to allow the store to pitch while the store center of gravity remains fixed in space. This situation was aggravated by the straight sting being used; normally offset stings (as shown in Fig. 1) are used to put the CTS close to the neutral or midrange position as regards the vertical movement. To correct for this nose-down pitching of the store caused by the local flow field of the model aircraft, unusually large ejector forces and strokes (and velocities) were required. These were as follows:

| Mach No. | Full-Scale Ejector Force, lb | Full-Scale Ejector Stroke, ft |
|---|---|---|
| 0.4 | 2,000 | 0.34 |
| 0.8 | 2,000 | 0.34 |
| 0.9 | 20,000 | 3.0 |
| 1.1 | 20,000 | 3.0 |
| 1.2 | 20,000 | 3.0 |

The implications of these unusually large ejector forces and strokes are discussed subsequently in Section 7.0.

## 5.0 ERROR ANALYSIS

An error analysis was performed to determine the uncertainties in the important test variables. The uncertainties in the tunnel flow parameters at a total pressure, $p_t$, of 1,200 psfa are as follows:

| Mach No. | $Up_t$, psfa | $UM_\infty$ | $Uq_\infty$, psfa |
|---|---|---|---|
| 0.4 | 9.7 | 0.0168 | 9.9 |
| 0.8 | 9.7 | 0.0094 | 7.6 |
| 0.9 | 9.7 | 0.0087 | 7.0 |
| 1.1 | 9.7 | 0.0079 | 5.8 |
| 1.2 | 9.7 | 0.0077 | 5.2 |

The uncertainties in the static aerodynamic coefficients are presented in Fig. 10 as a function of free-stream Mach number for three values of each coefficient. These uncertainties are determined for a 95-percent confidence level.

No simple method exists for evaluating the effects of test variable uncertainties on the trajectory of the store. These uncertainties not only vary with Mach number and total pressure but with position and attitude of the store. Deviations from the true trajectory are the result of timewise integrations of all of these uncertainties. The reader is directed to Ref. 3 for an appraisal of how fixed uncertainties or biases in the store aerodynamic and inertial characteristics, and in other significant test parameters, can affect the store motion.

## 6.0 TEST RESULTS

The trajectories obtained with varying sting length are presented for each Mach number in Fig. 11 for the finned store and for each Mach number in Fig. 12 for the unfinned store. The configurations are identified in these figures with the following designations:

| Configuration Number | Fin Status | Nominal Sting Length, in. | Actual Sting Length (Fig. 9), in. |
|---|---|---|---|
| 1 | Finned | 3 | 2.984 |
| 2 | Unfinned | 3 | 2.984 |
| 3 | Finned | 5 | 4.984 |
| 4 | Unfinned | 5 | 4.984 |
| 5 | Finned | 7 | 6.984 |
| 6 | Unfinned | 7 | 6.984 |
| 7 | Finned | 13 | 12.984 |
| 8 | Unfinned | 13 | 12.984 |

In these figures the orthogonal distances (XP, YP, ZP) of the store center of gravity from the carriage position in axes that are parallel to the aircraft model axes, the pitching deviations (DTHA), and yawing-moment deviations (DPSI) from the carriage position are presented as functions of time. Also presented in these figures are plots of pitching deviations (DTHA) versus vertical distance (ZP) with respect to the carriage position.

The results of the vertical grid traverses are presented for each Mach number in Fig. 13 for the finned store and in Fig. 14 for the unfinned store. Again in these figures, sting length is the parameter for the separate curves. The data presented in Figs. 13 and 14 are the store static aerodynamic coefficients versus vertical distance from the carriage position. In Figs. 11 through 14, only every fourth data point is plotted; however, every data point is connected by straight lines as is readily apparent in the grid traverse plots.

As stated earlier, free-stream yaw traverses were performed at the maximum vertical distance away from the aircraft model and as far foward as the CTS would permit to minimize any possible influence of the aircraft model on the flow field at the store location. An examination of the normal-force and pitching-moment coefficients (which would be expected to be constant over the yaw traverses) showed variations in coefficients equivalent to angle-of-attack variations of three degrees and more at all Mach numbers. This change in the pitch plane coefficients with angle of yaw indicated that the stores were still in an interference flow field of the aircraft model. Therefore, the "free-stream" results are not presented in this report.

Measurements of the store base pressure were obtained and generally showed an increase in base pressure attributable to shortening of the sting length; however, because of instrumentation difficulties the data, as a whole, were too erratic and are not included in this report.

## 7.0 DISCUSSION

Examination of the results presented in Figs. 11a through e for the finned store shows only small differences in the trajectory variables for the different sting lengths at the subsonic Mach numbers and virtually no difference at supersonic speeds. The same is true for the unfinned store as represented by the data in Figs. 12a through e. The most significant differences in the trajectories for the various sting lengths occurred at 0.9 in the yawing motion (DPSI) and the pitching motion (DTHA). The differences in trajectories were remarkably small when one considers the length of sting variation of from about 5 in. to 15 in. between the model base and the apex of the CTS cone. Even more surprising is the fact that when the two shorter stings were used the CTS cone was abreast of the aircraft model afterbody. At $M_\infty$ = 0.8 and 0.9 it is likely that local interference (or choking) may have occurred between the CTS head and the aircraft model after-fuselage which could have altered the flow field at the store. Throughout the data in these figures there are differences in XP versus time caused by the axial-force differences which resulted from sting-induced base-drag changes. Note that increased XP movement is associated with long stings. XP was probably the least significant of the trajectory variables as regards store separation, and ordinarily corrections to the axial force (and the resultant XP motion) caused by base pressure variations are not attempted. An argument that might be used to explain these small differences in the trajectories is that the unusually large ejector forces moved the stores out of the flow field of the aircraft model in so short a time that the aerodynamic interference effects of the various stings did not persist long enough to have an effect on the motion. This argument could be valid only for Mach numbers 0.9 and higher where the unusually large ejector forces were used. Even if this argument were valid, the interferences would still be evident in the grid traverses.

Examination of the grid traverses presented in Figs. 13a through e for the finned model and 14a through e for the unfinned model again shows only small differences between the various sting lengths. The differences in axial-force coefficients were most pronounced especially at the higher subsonic Mach numbers, but nonexistent at the supersonic Mach numbers (for both models). Again the only noteworthy differences in the grid data were at $M_\infty = 0.90$. For this Mach number, there was a significant difference in magnitude and shape of the curves for the static stability coefficients in both the pitch and yaw planes. The differences were greatest close to the carriage position. These differences again were very likely attributable to an interference effect between the CTS head and the aircraft model after-fuselage. It should be noted in Figs. 12c and 13c that the change in side-force coefficient, $C_y$, from the long sting to the two shortest stings was in the direction of an increased spanwise flow from root to tip, which could have been caused by a flow restriction or choking condition inboard of the store.

At all other Mach numbers the differences in grid data were small and within the measurement uncertainties presented in Fig. 9 (except for the axial-force coefficients). At supersonic speeds, there were no significant differences in the grid data even for the axial-force coefficient.

## 8.0 CONCLUSIONS

The conclusion that may be drawn from the results of this test is that the CTS exerts a negligible effect on the separation trajectories on "typical" stores for stings of practical lengths. Even in the case of the two shorter stings (nominally 3 and 5 in. long) used in this test, interference effects of the CTS were not large. This result was surprising in that the lengths were chosen intentionally to produce interference effects. In addition, an interference effect was observed on axial force, as expected, and occurred in a quite systematic manner.

A recommended follow-on test to substantiate these results should utilize a bent or offset sting as is customarily used in store separation testing.

## REFERENCES

1. Christopher, J. D. and Carleton, W. E. "Captive-Trajectory Store-Separation System of the AEDC-PWT 4-Foot Transonic Tunnel." AEDC-TR-68-200 (AD839743), September 1968.

2. Dix, R. E. "Influences of Sting Support on Aerodynamic Loads Acting on Captive Store Models." AEDC-TR-76-1 (AFATL-TR-76-25) (AD-A022257), March 1976.

3. Marshall, John C. and Summers, Willard E. "An Analysis of the Relative Importance of Parameters Required for the Simulation of Store Separation Trajectories." Paper presented at the Aircraft/Stores Compatibility Symposium, Dayton, Ohio, December 7-9, 1971.

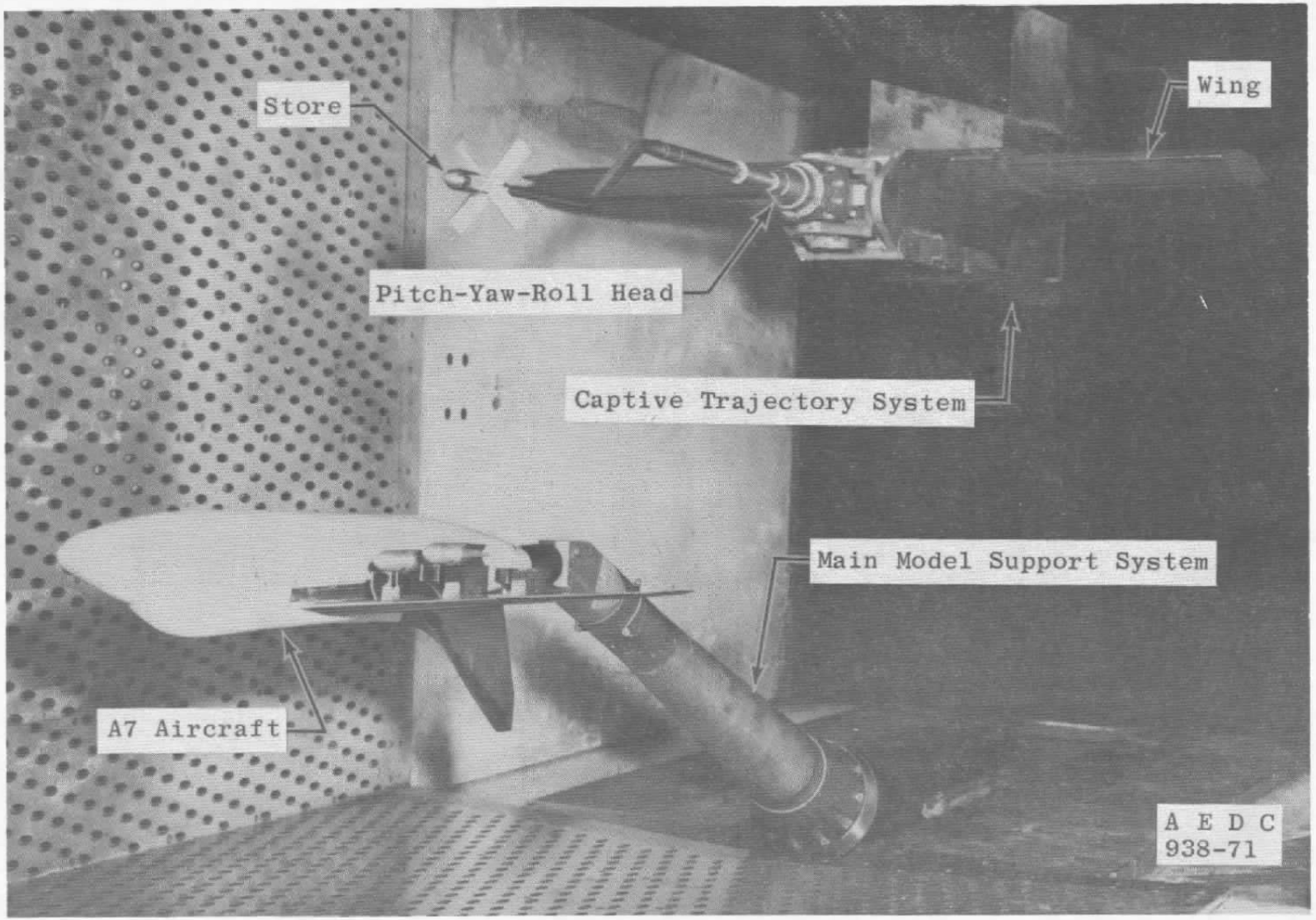


Figure 1. Photograph of a typical store separation test installation.

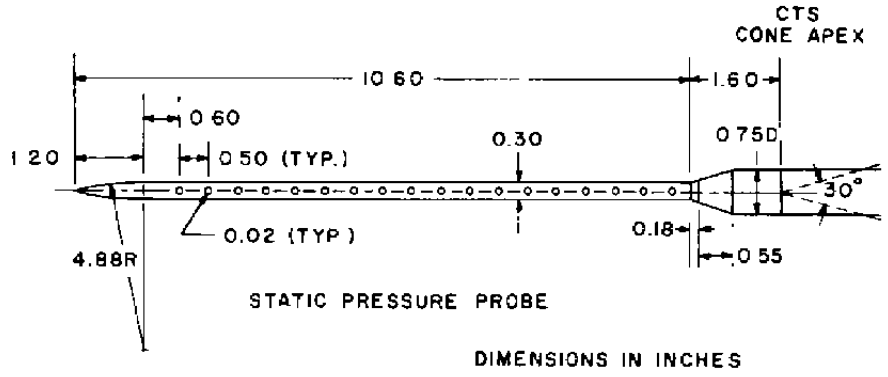


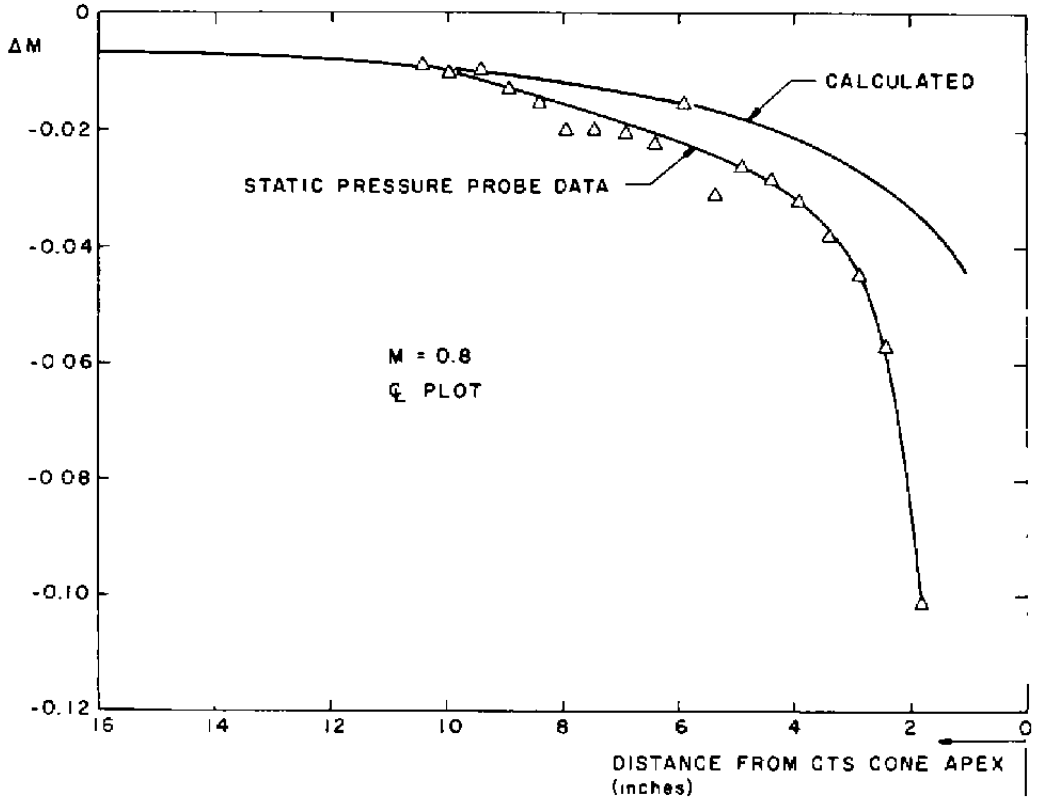


**Figure 2. Change in local Mach number attributable to support system interference.**

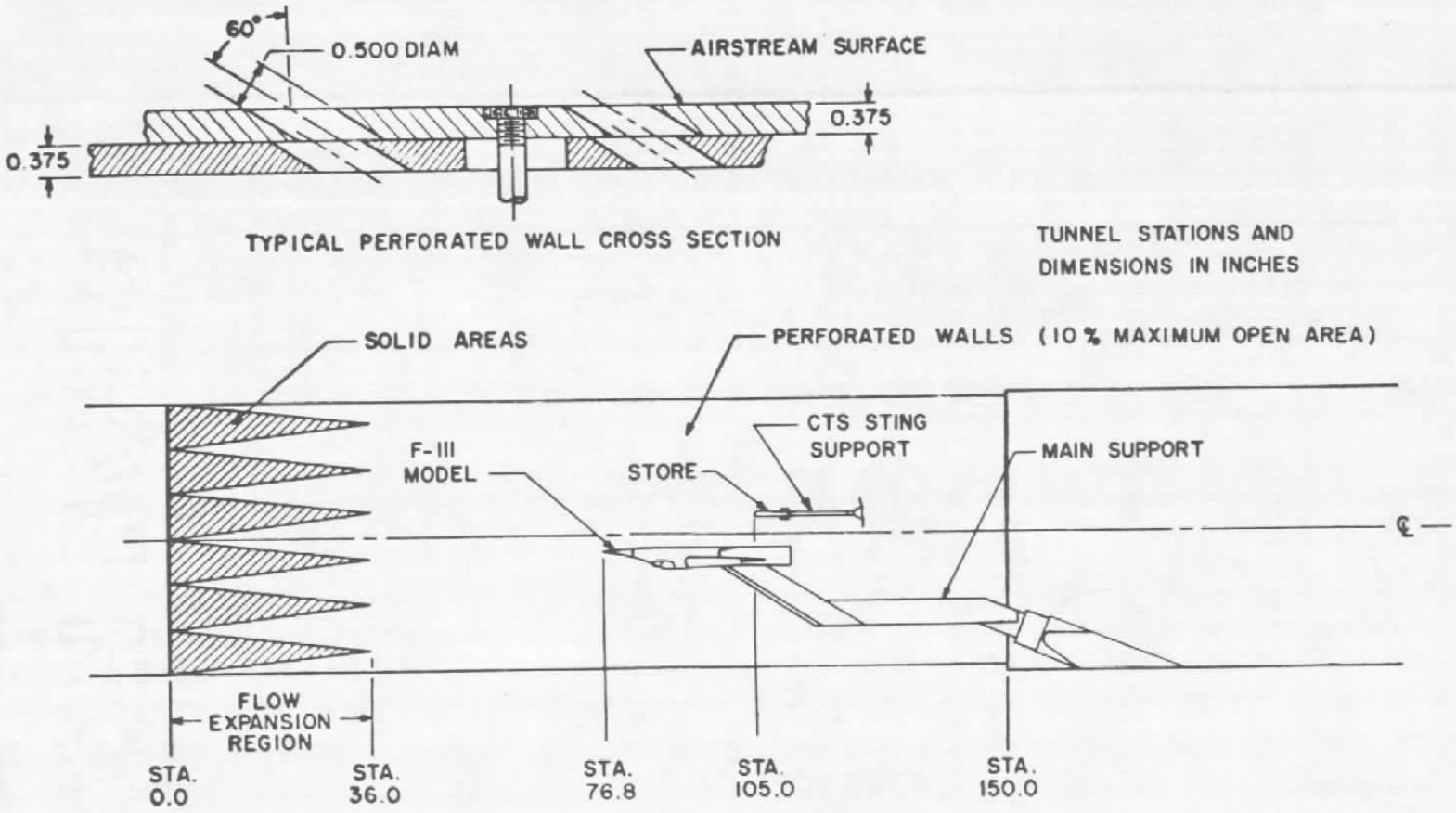


Figure 3. Sketch of F-111 installation.

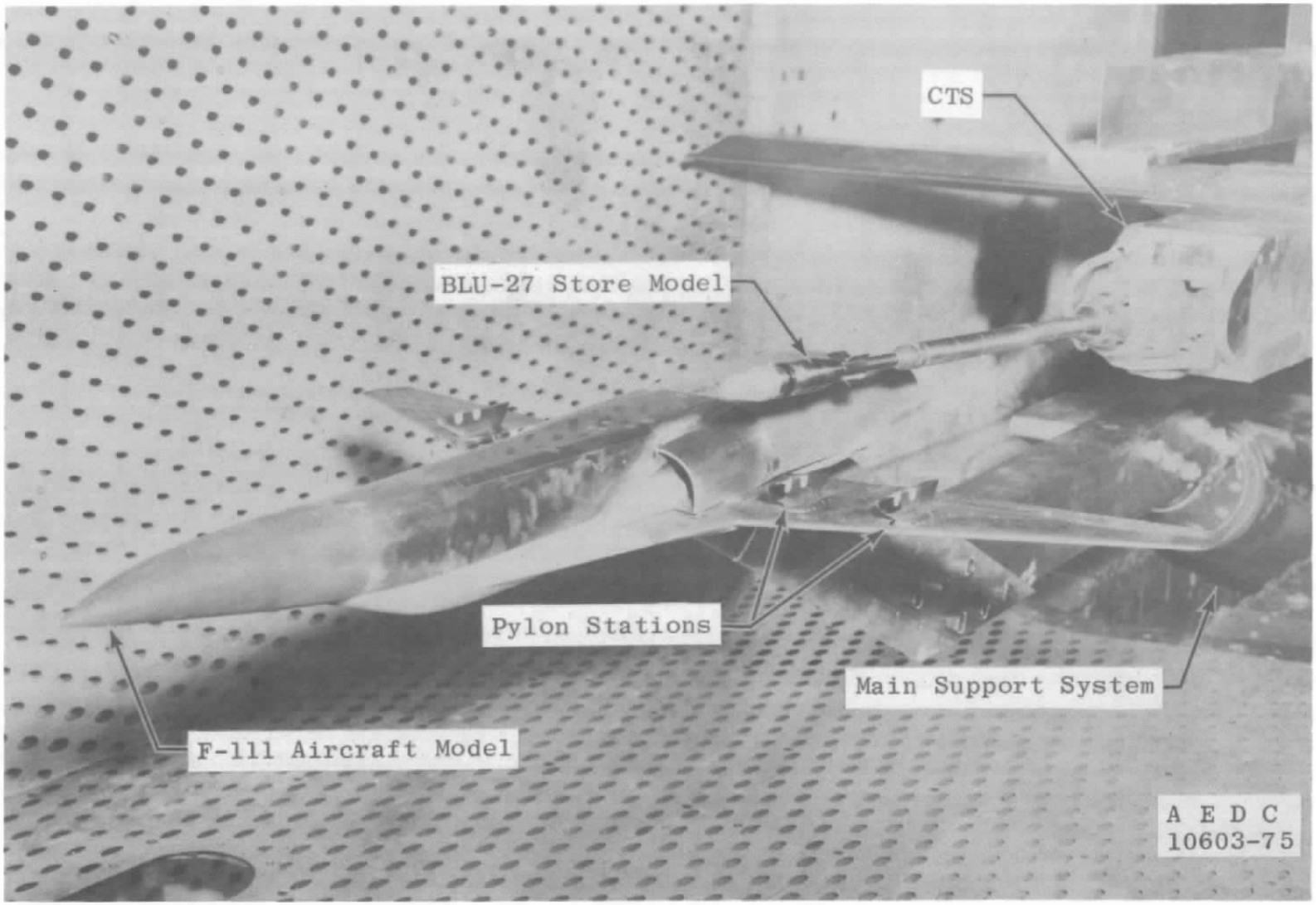


Figure 4. Photograph of the test installation.

NOSE COORDINATES

| STA | DIAM |
|---|---|
| 0 000 | 0 060 |
| 0.020 | 0 105 |
| 0 045 | 0 152 |
| 0 095 | 0 222 |
| 0 145 | 0 275 |
| 0 245 | 0 359 |
| 0 345 | 0 434 |
| 0 445 | 0 502 |
| 0 533 | 0 558 |

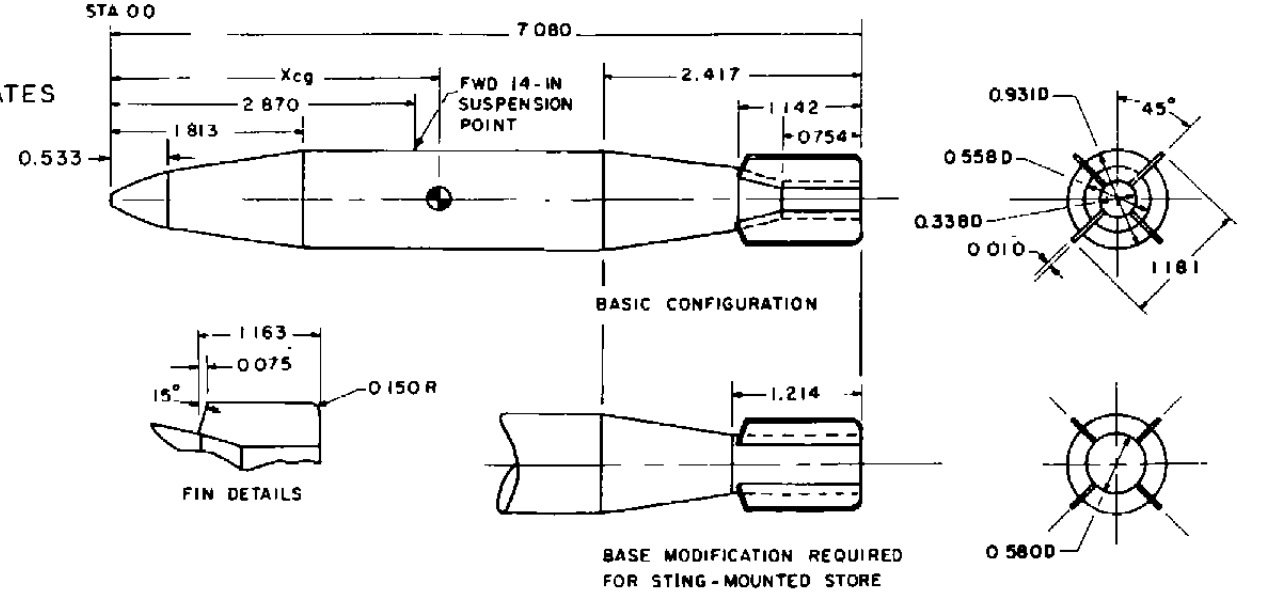


DIMENSIONS IN INCHES

Figure 5. Modified 1/20-scale finned BLU-27B/B model.

NOSE COORDINATES

| STA | DIAM |
|---|---|
| 0 000 | 0.060 |
| 0 020 | 0 105 |
| 0 045 | 0.152 |
| 0 095 | 0 222 |
| 0 145 | 0 275 |
| 0 245 | 0.359 |
| 0 345 | 0 434 |
| 0 445 | 0 502 |
| 0 533 | 0 558 |

AFTERBODY COORDINATES

| | |
|---|---|
| 5.943 | 0 558 |
| 6 031 | 0.502 |
| 6.131 | 0 434 |
| 6.231 | 0.359 |
| 6.331 | 0 275 |
| 6 381 | 0 222 |
| 6.431 | 0.152 |
| 6.456 | 0 105 |
| 6 476 | 0 060 |

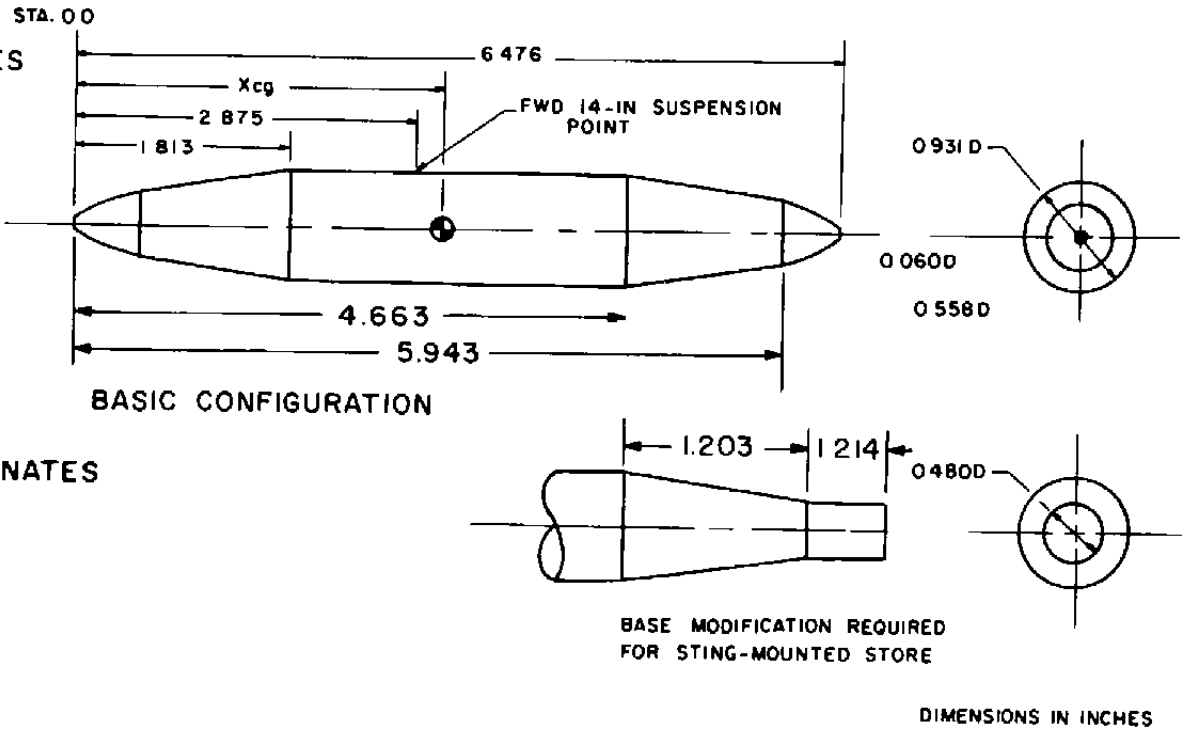


Figure 6. Modified 1/20-scale unfinned BLU-27B/B model.

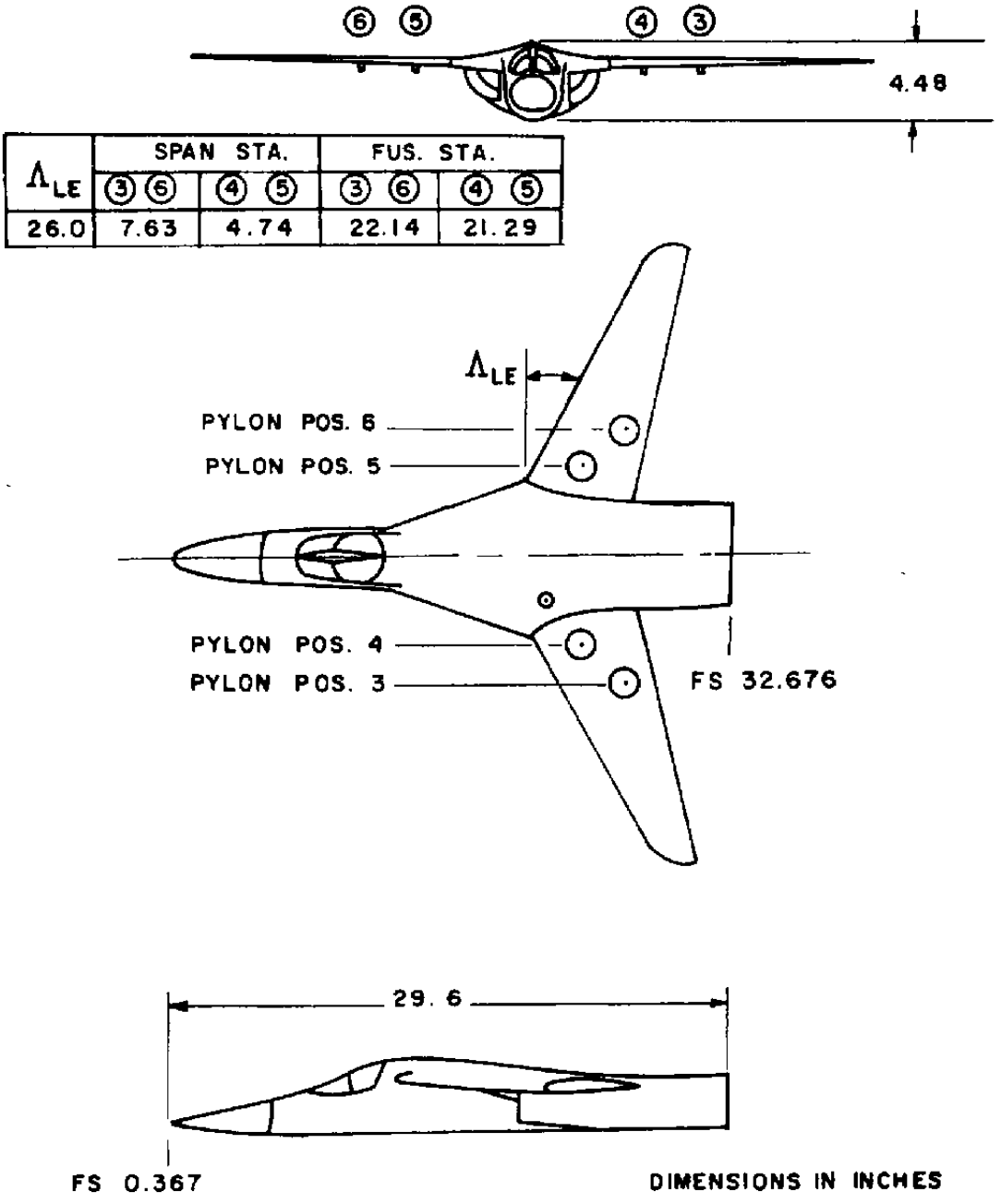


| $\Lambda_{LE}$ | SPAN STA. | | FUS. STA. | |
|---|---|---|---|---|
| | ③ ⑥ | ④ ⑤ | ③ ⑥ | ④ ⑤ |
| 26.0 | 7.63 | 4.74 | 22.14 | 21.29 |

Figure 7. Sketch of 1/24-scale F-111 aircraft model.

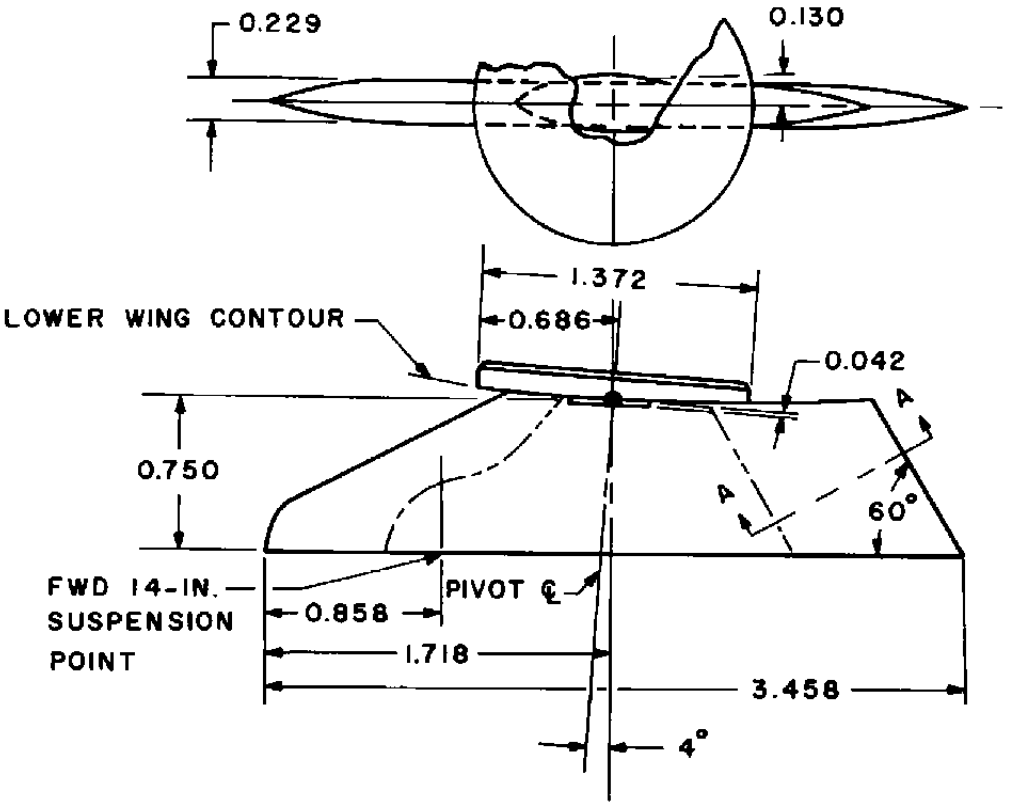


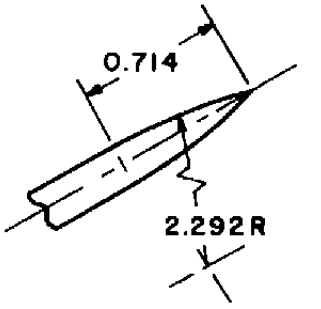


DIMENSIONS IN INCHES

Figure 8. Sketch of 1/24-scale outboard pylon.

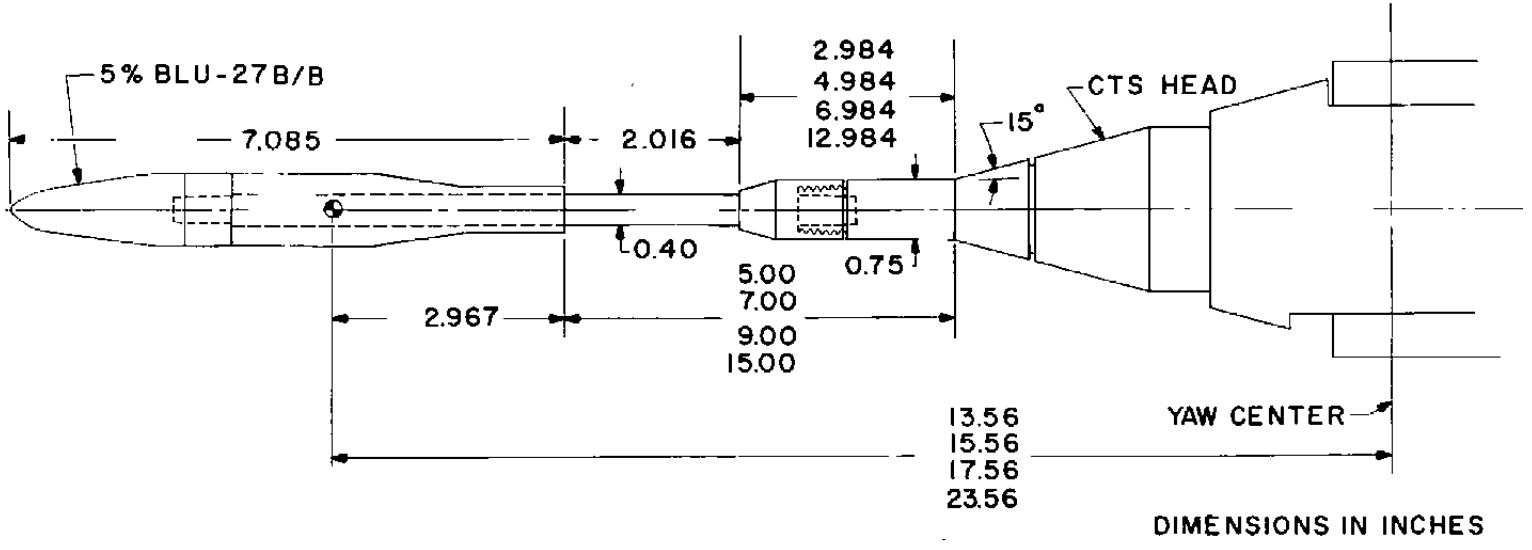


Figure 9. Sketch of unfinned BLU-27B/B installed on CTS sting.

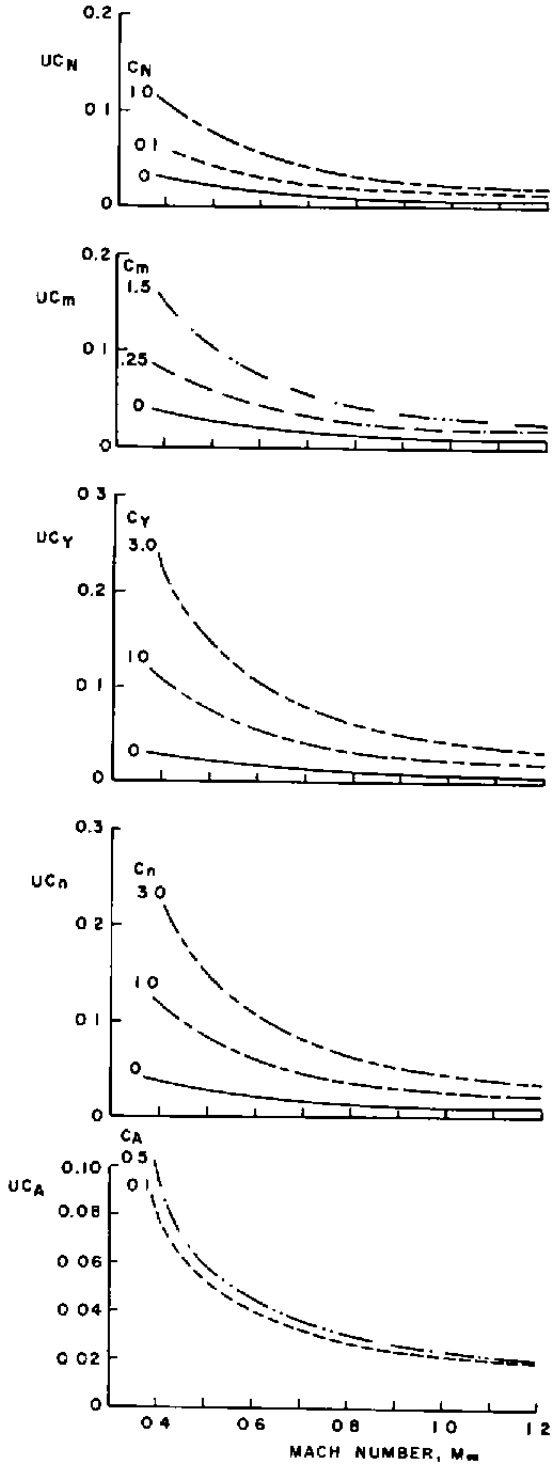


Figure 10. Uncertainties in the static aerodynamic coefficients versus Mach number, $p_t$ = 1,200 psfa.

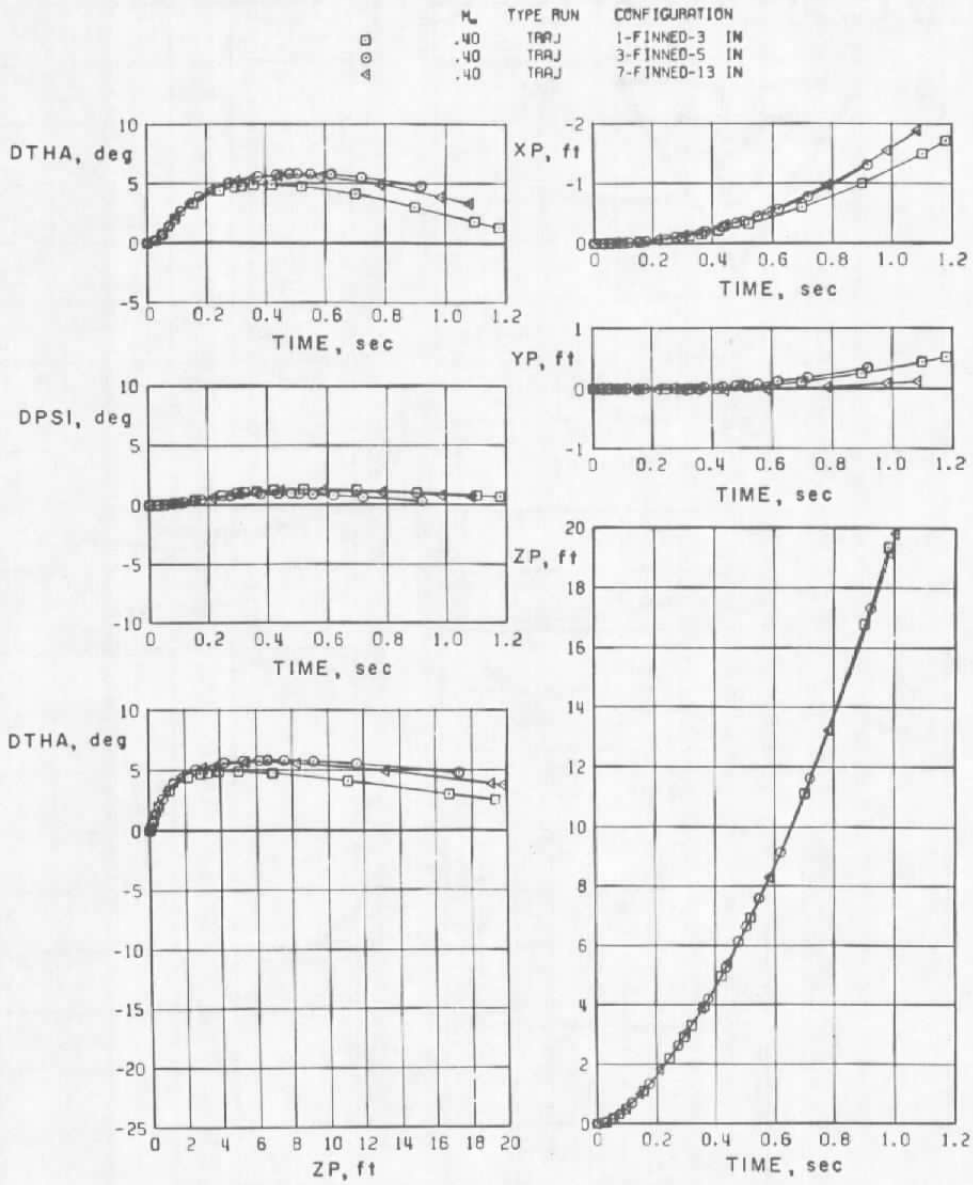


a. $M_\infty = 0.40$

**Figure 11. Trajectories of the finned BLU-27B/B using various sting lengths.**

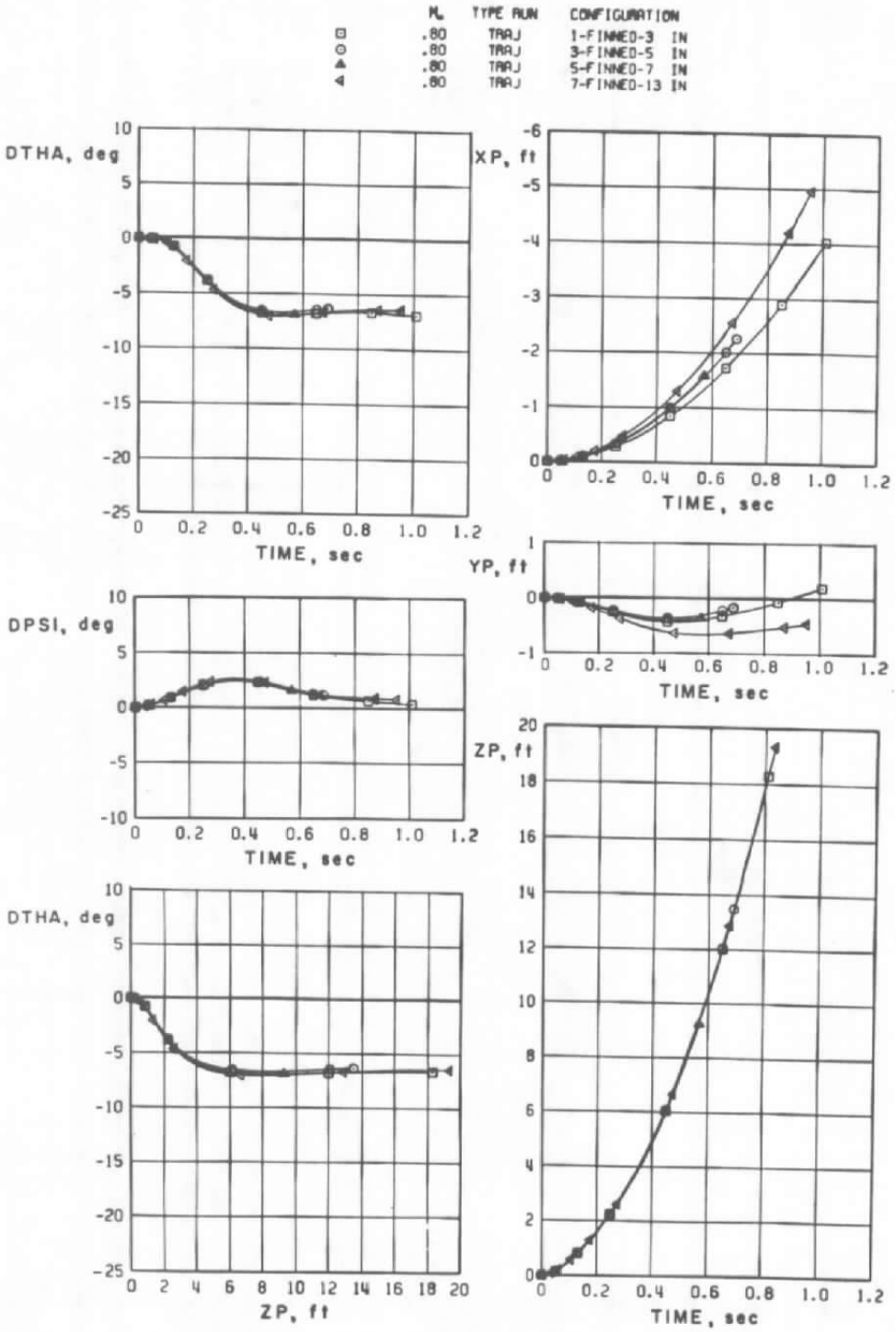


b. $M_\infty = 0.80$

Figure 11. Continued.

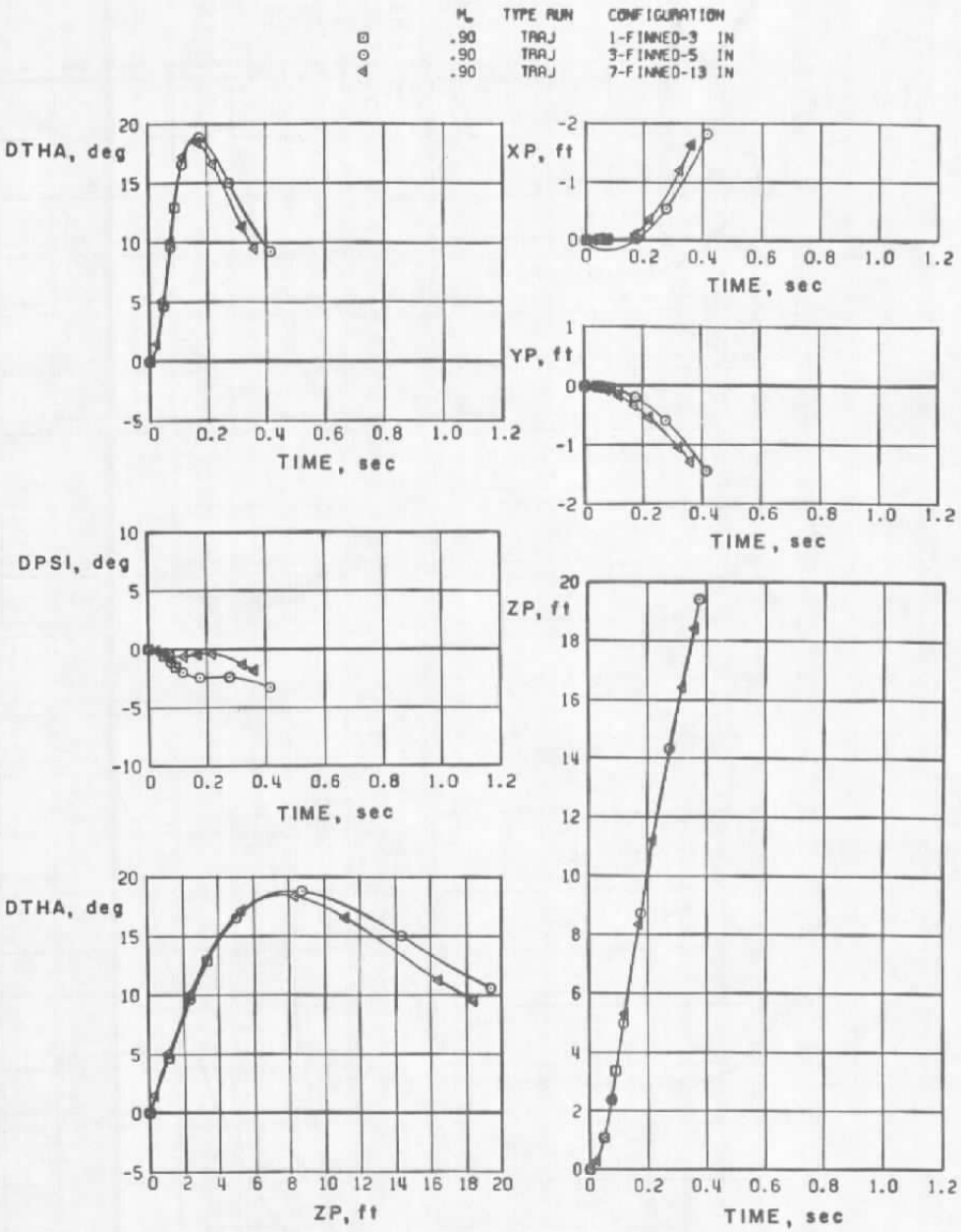


c. $M_\infty = 0.90$

**Figure 11. Continued.**

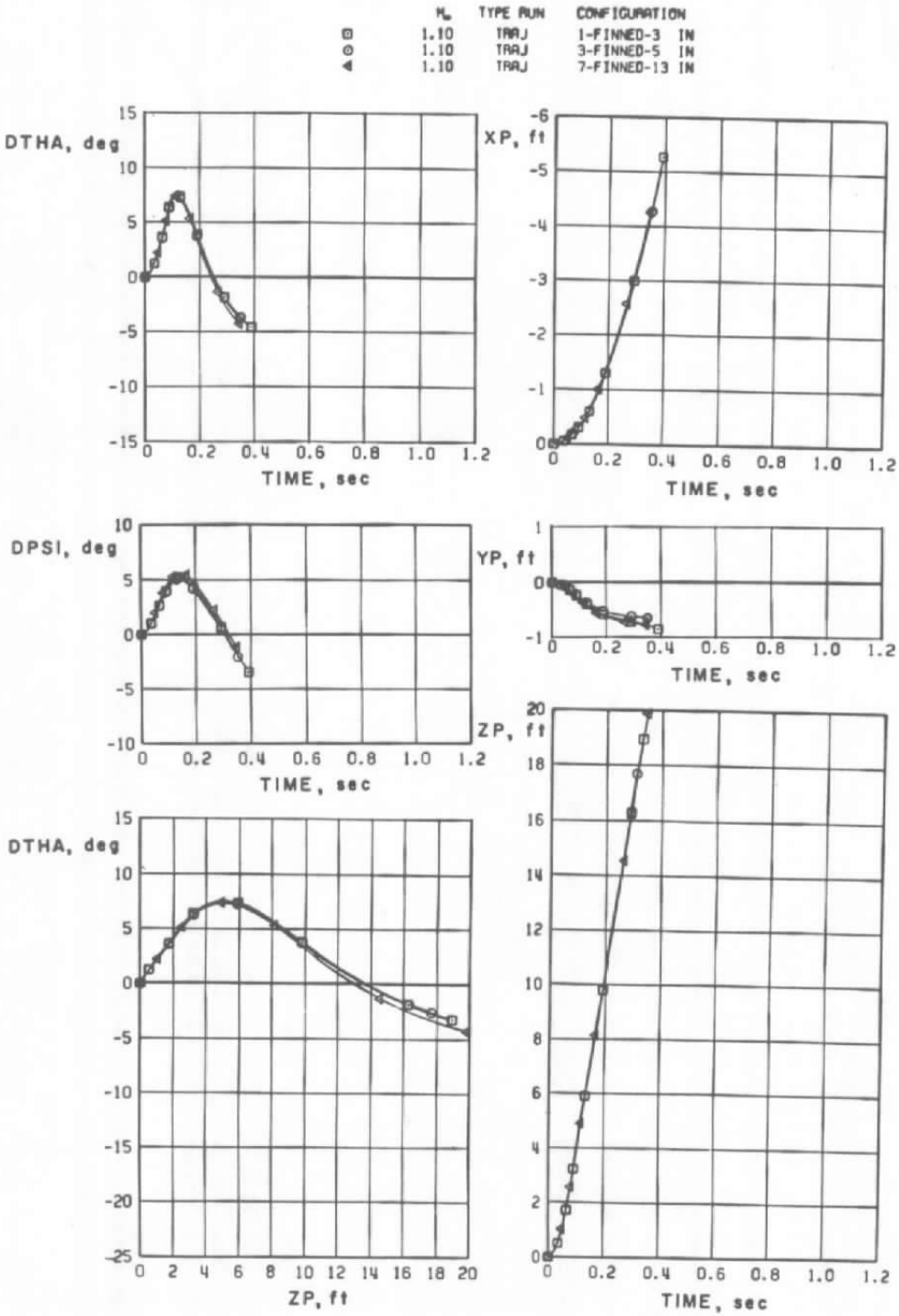


d. $M_\infty = 1.10$

Figure 11. Continued.

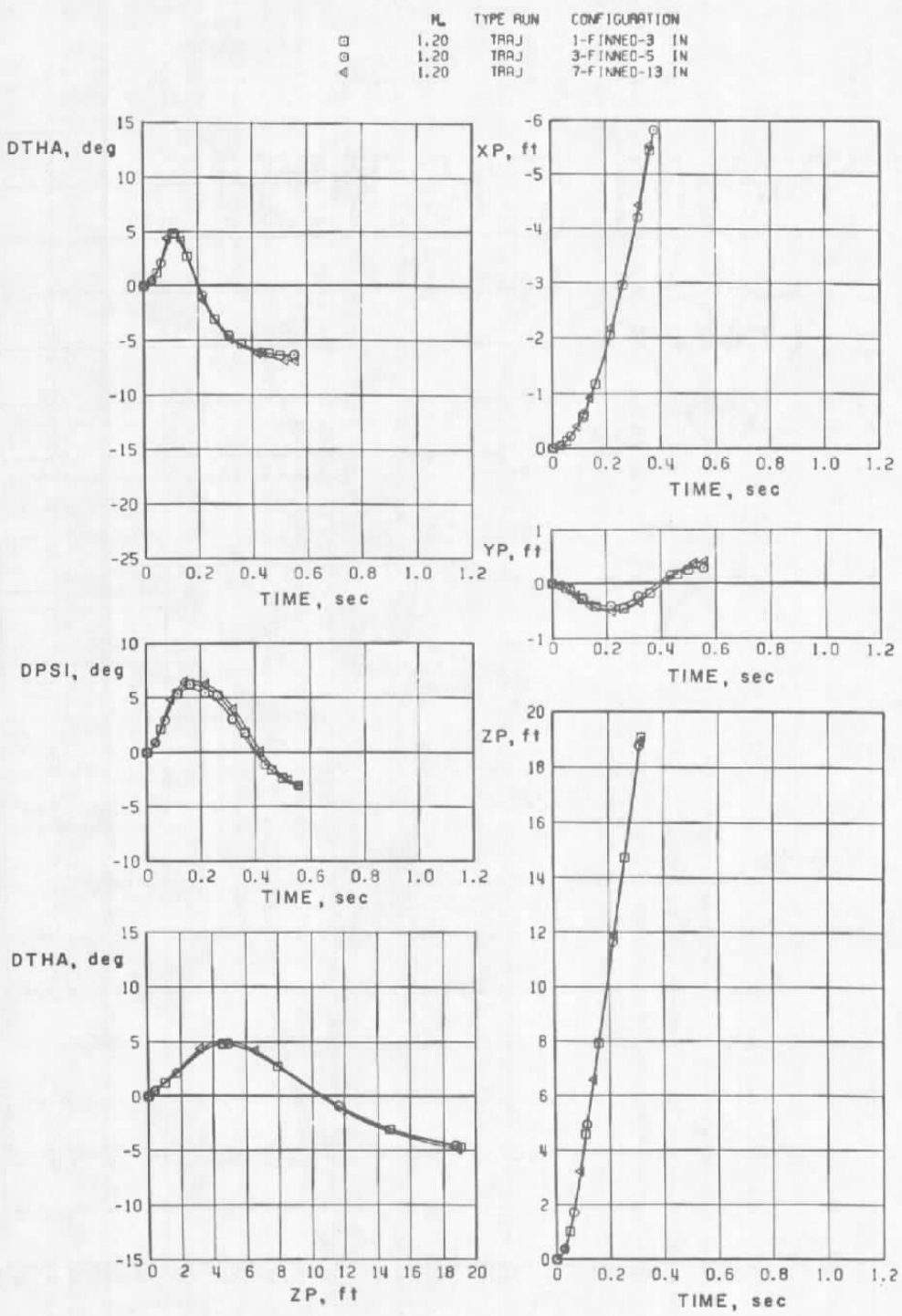


e. $M_\infty = 1.20$

**Figure 11. Concluded.**

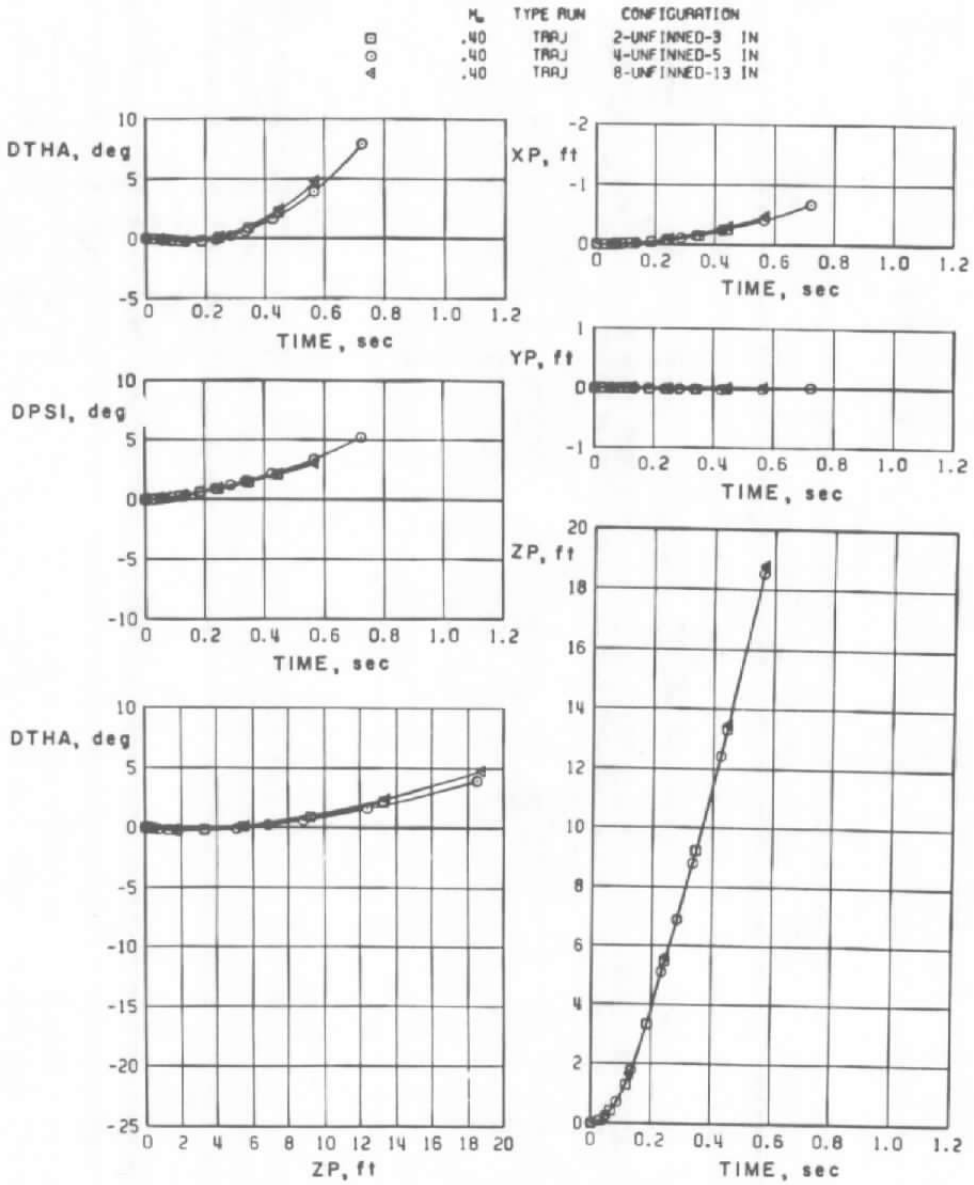


a. $M_\infty = 0.40$

**Figure 12. Trajectories of the unfinned BLU-27B/B using various store lengths.**

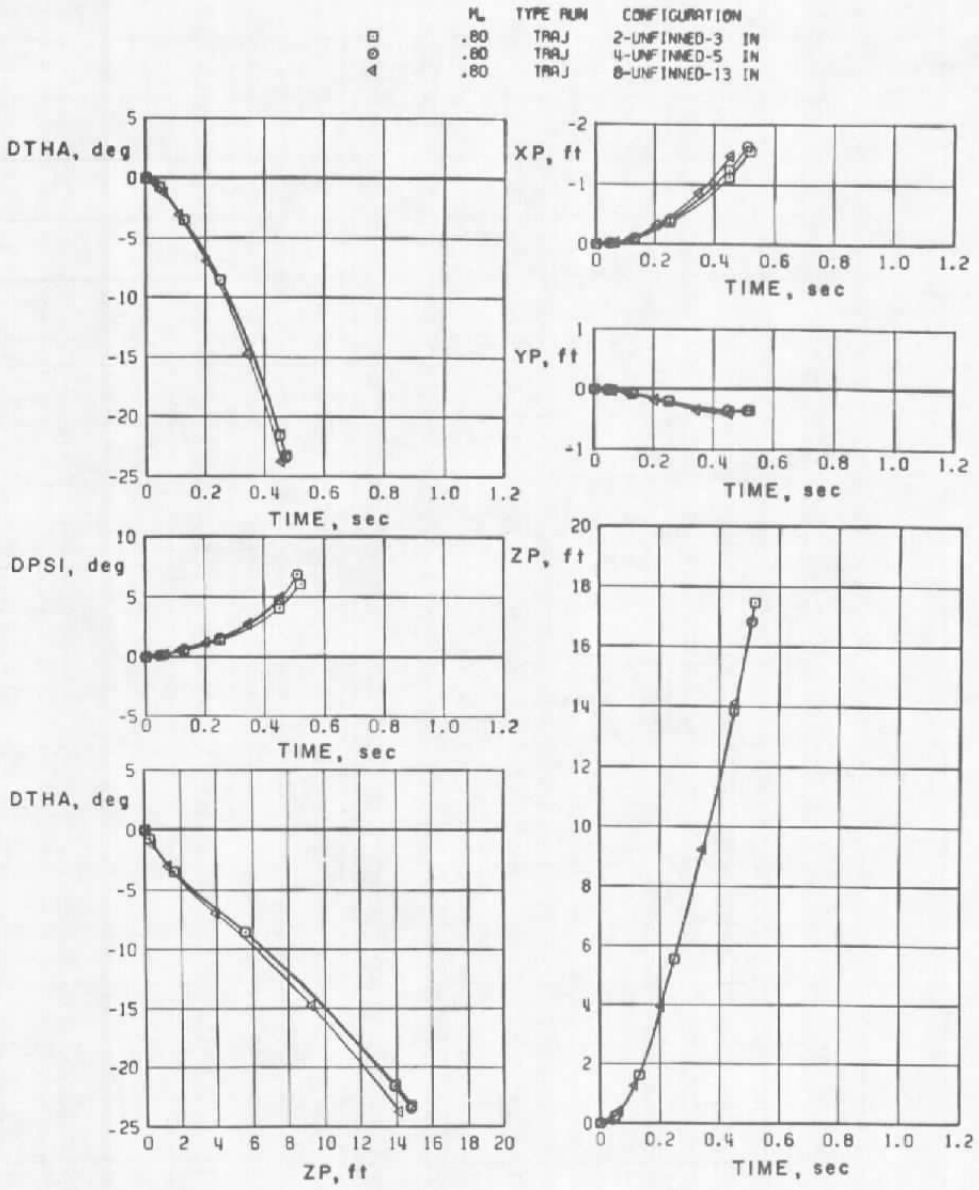


b. $M_\infty = 0.80$

**Figure 12. Continued.**

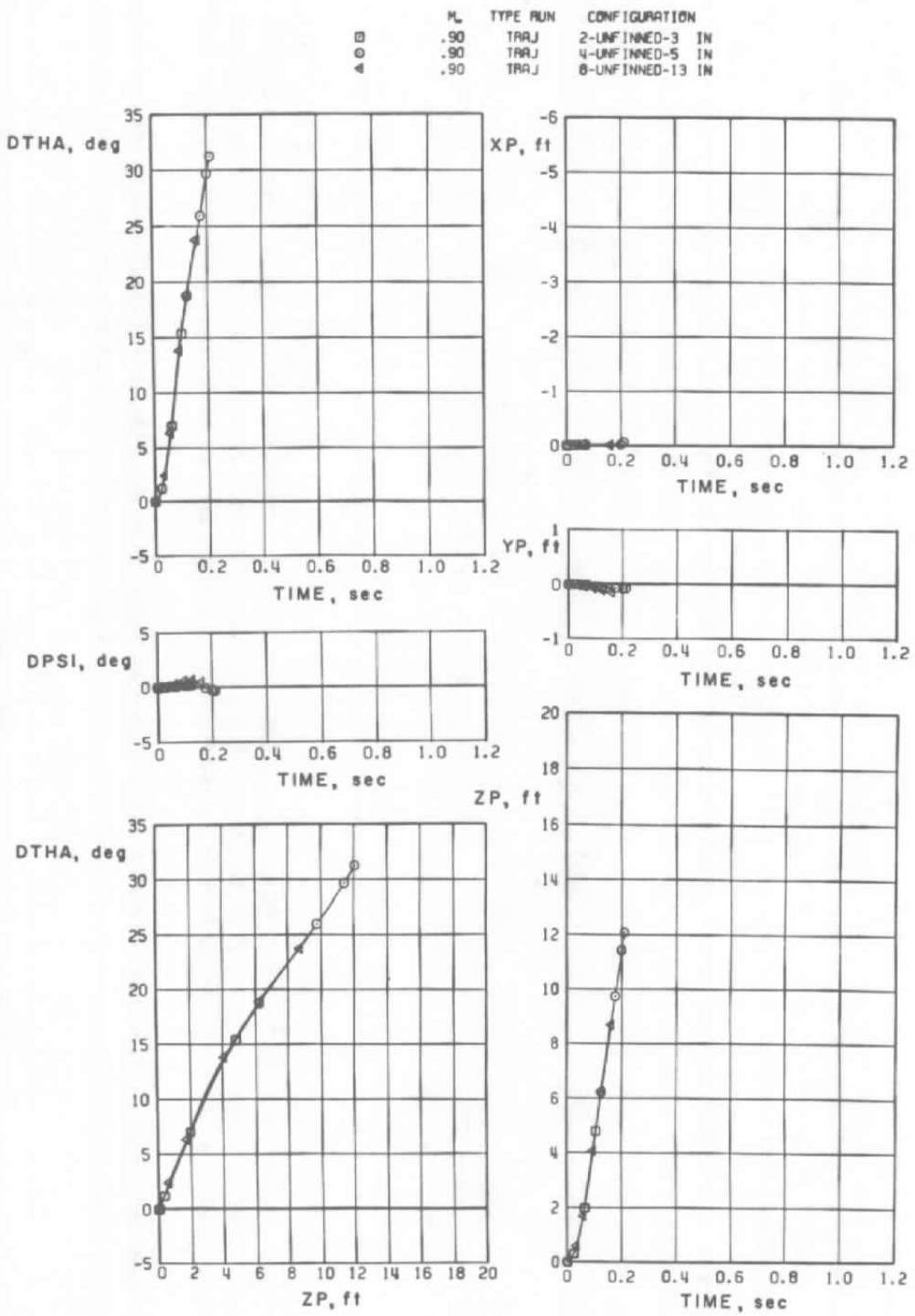


c. $M_\infty = 0.90$

Figure 12. Continued.

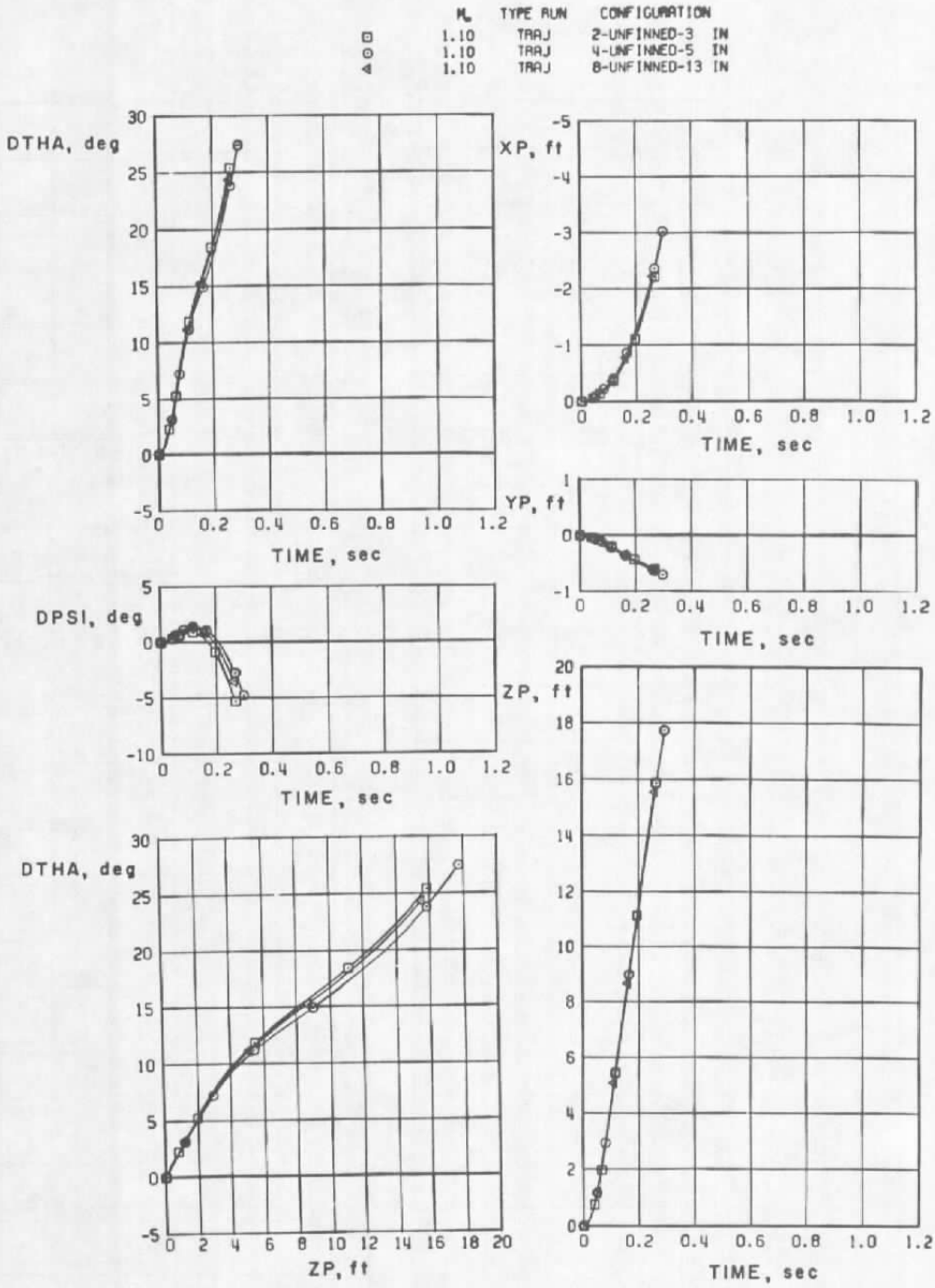


d. $M_\infty = 1.10$

**Figure 12. Continued.**

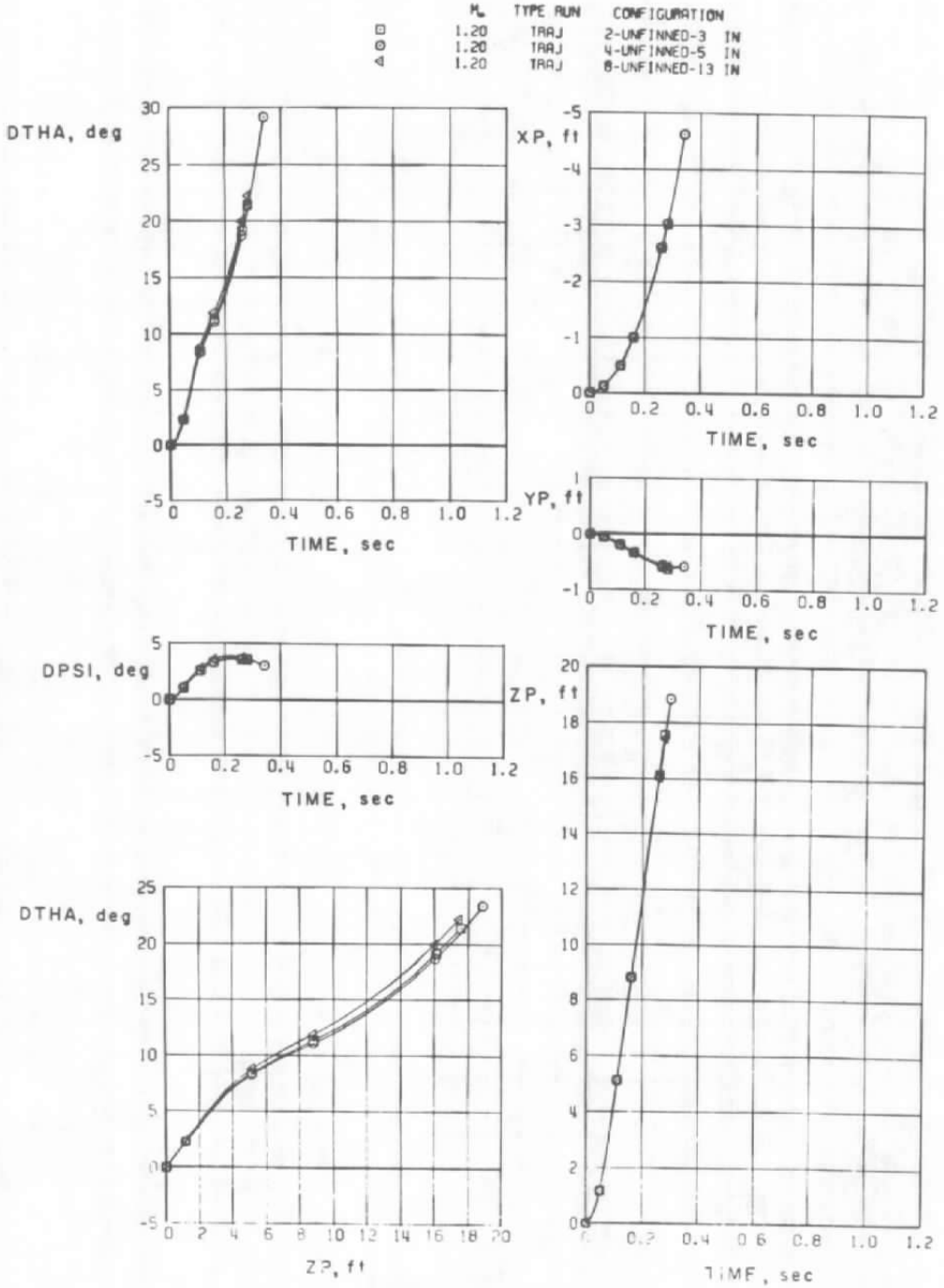


e. $M_\infty = 1.20$

**Figure 12. Concluded.**

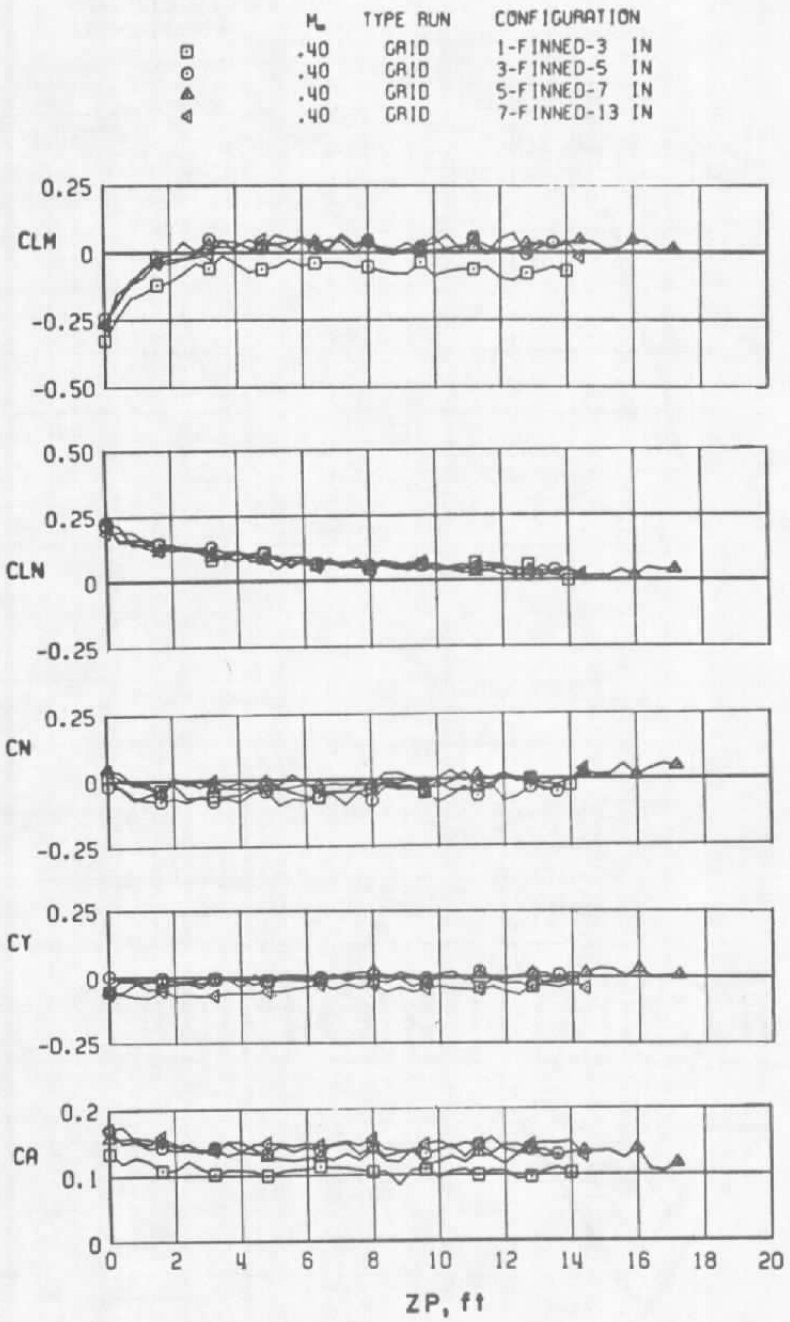


a. $M_\infty = 0.40$

**Figure 13. Grid traverses of the finned BLU-27B/B.**

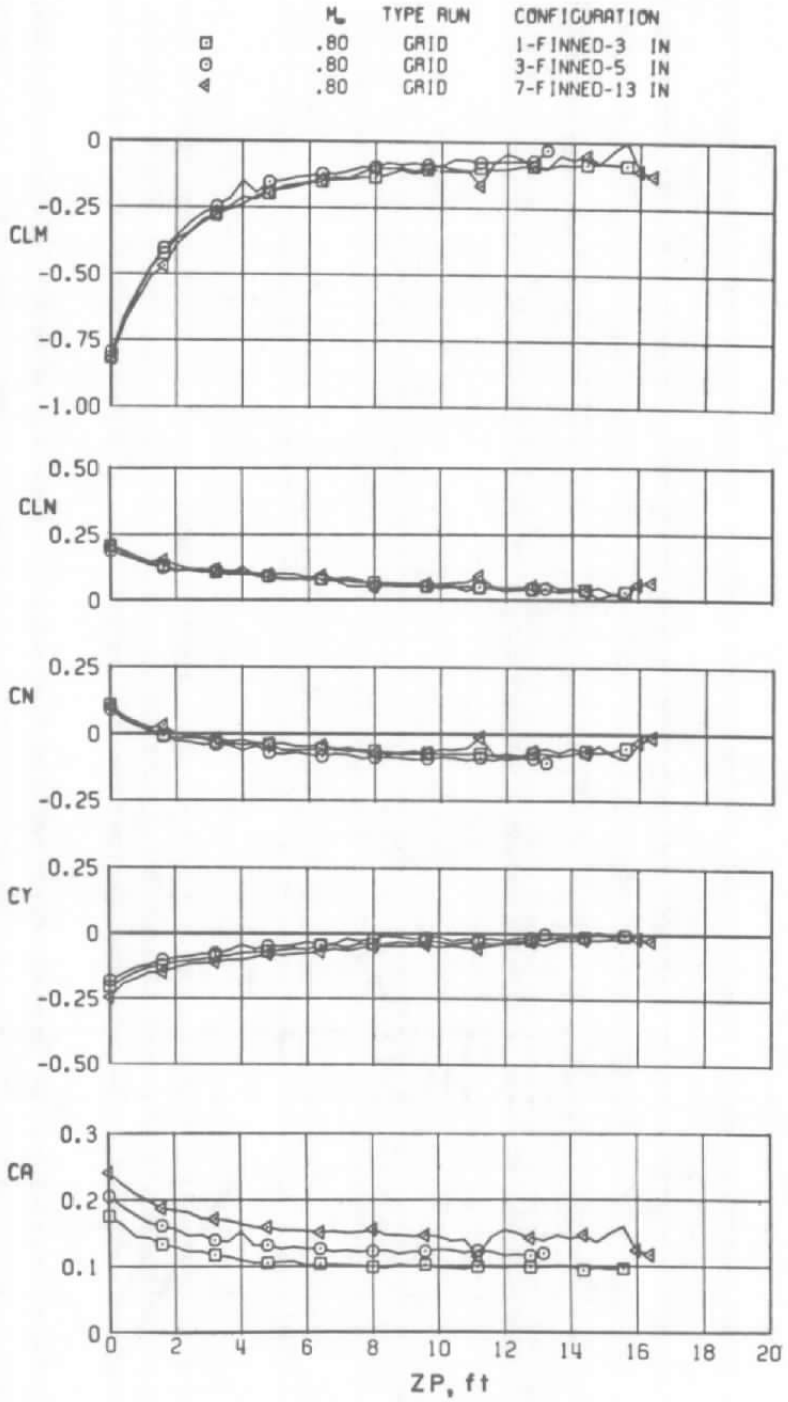


b. $M_\infty = 0.80$

Figure 13. Continued.

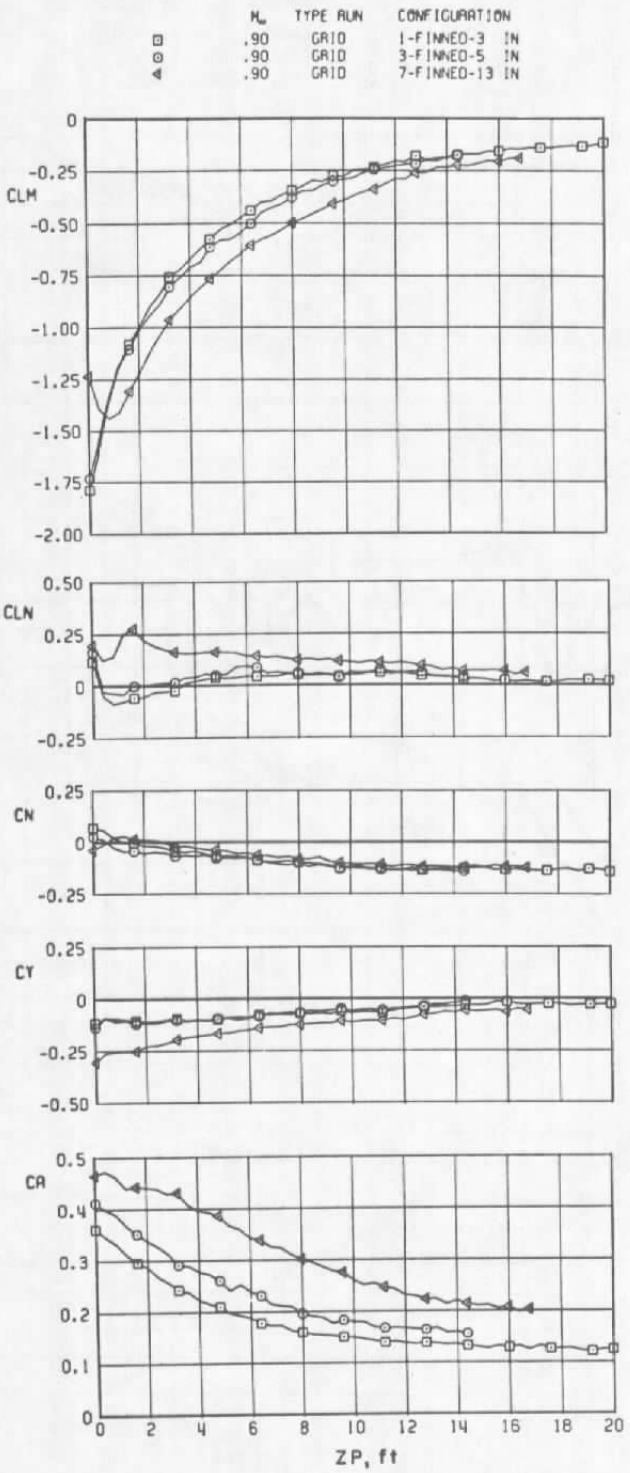


c. $M_\infty = 0.90$

**Figure 13. Continued.**

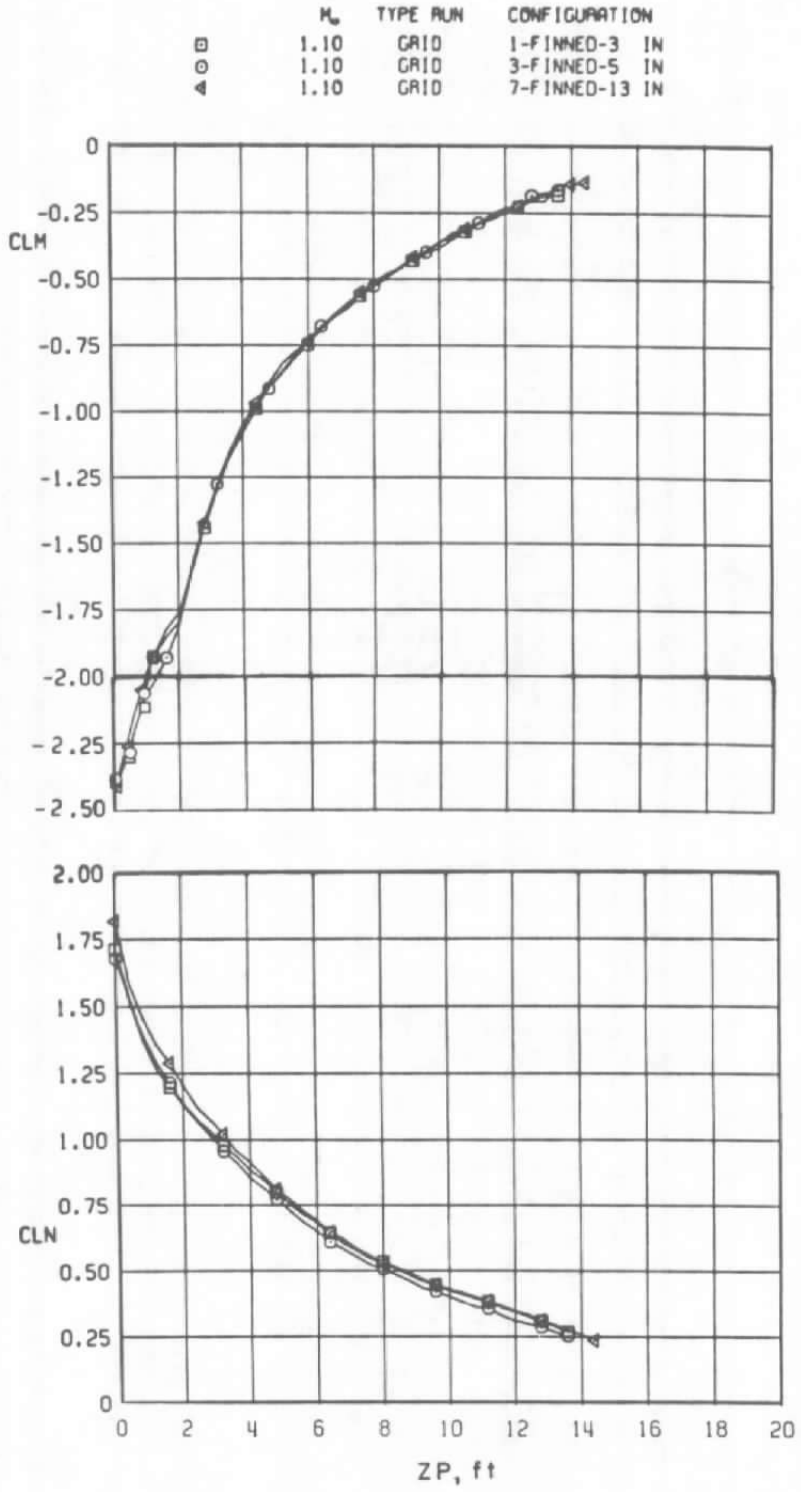


d. $M_\infty = 1.10$

Figure 13. Continued.

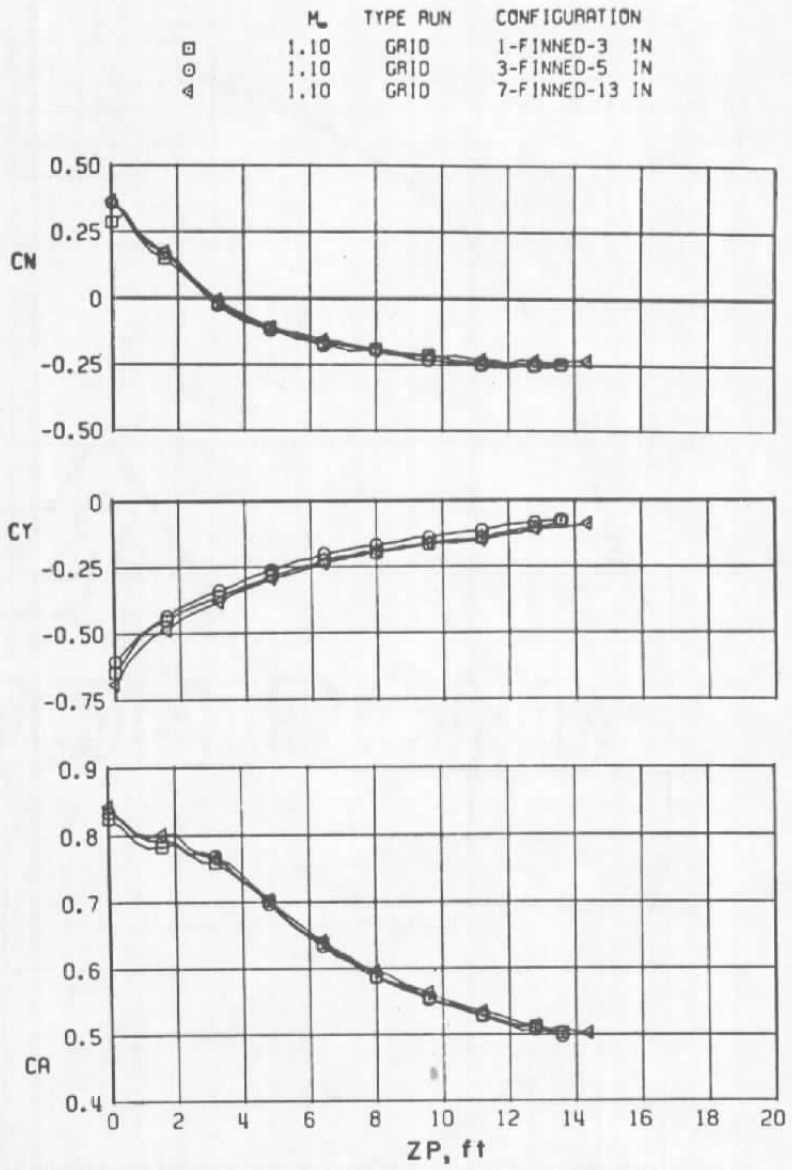


d. Concluded
Figure 13. Continued.

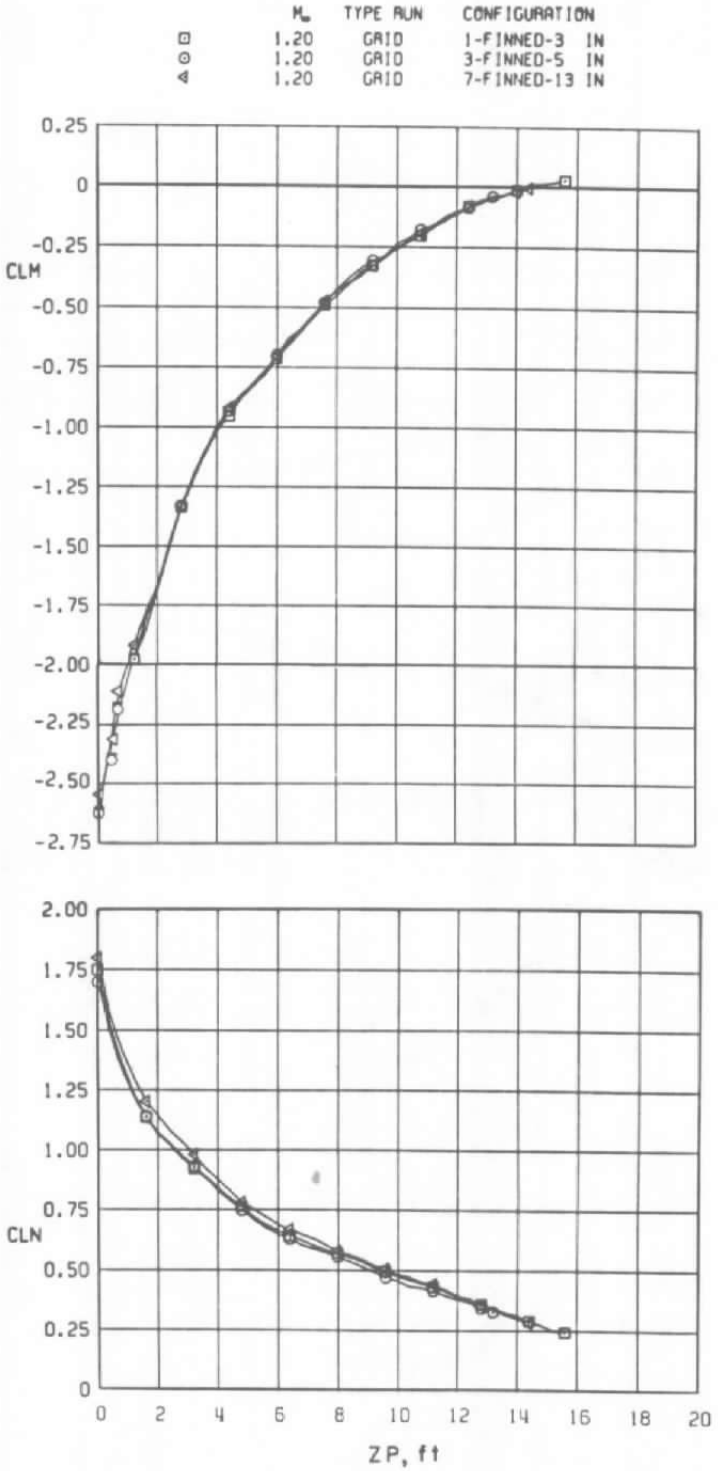


e. $M_\infty = 1.20$

**Figure 13. Continued.**

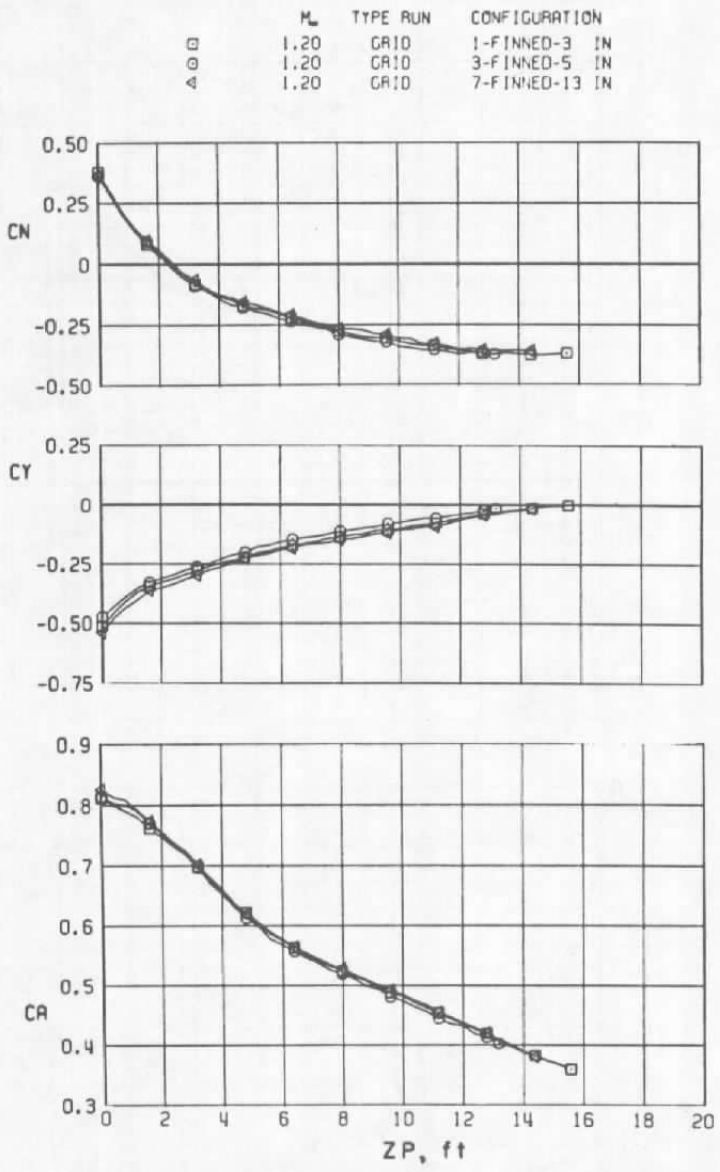


e. Concluded

**Figure 13. Concluded.**

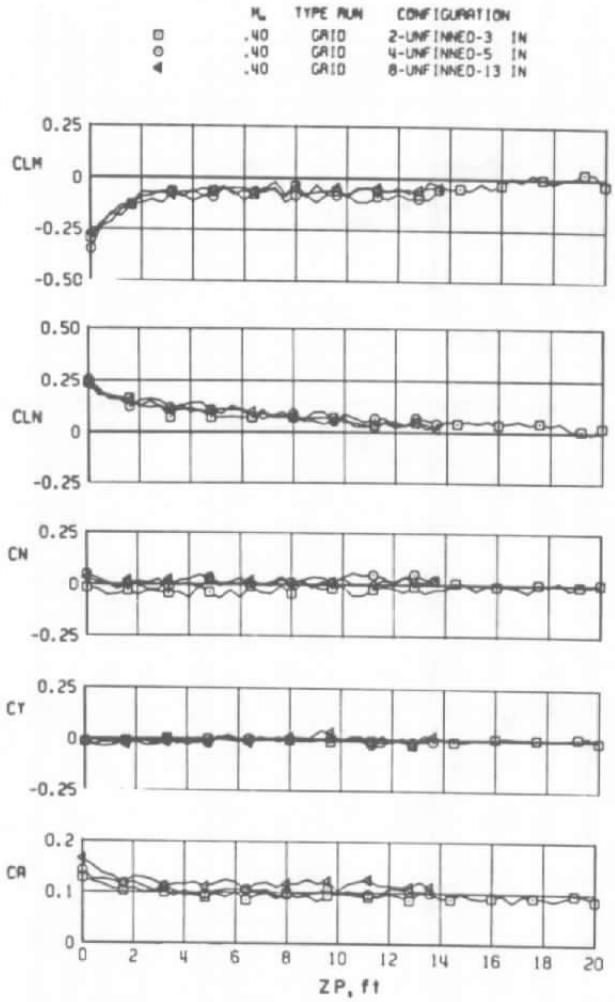


a. $M_\infty = 0.40$

**Figure 14. Vertical traverses of the unfinned BLU-27B/B.**

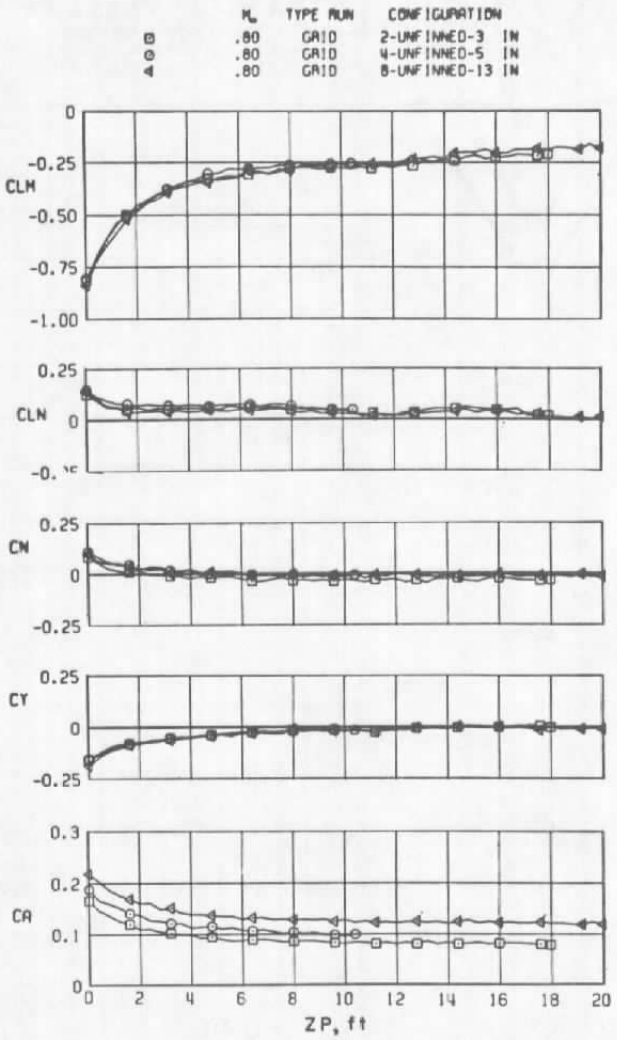


b. $M_\infty = 0.80$

**Figure 14. Continued.**

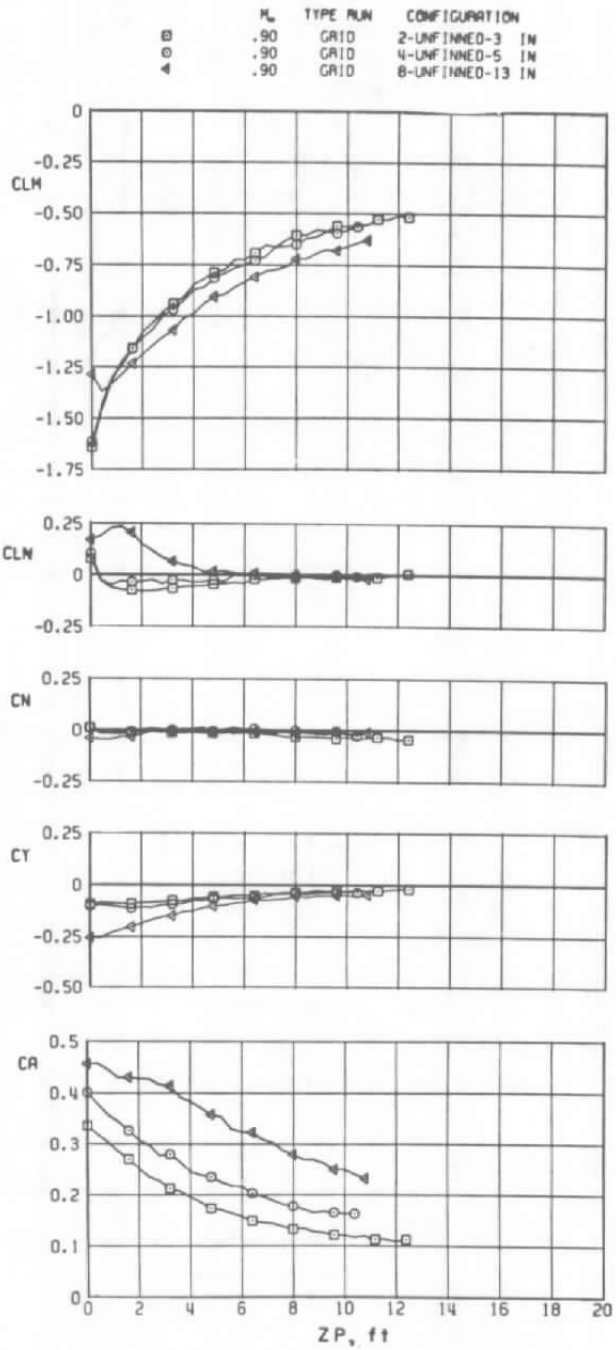


c. $M_\infty = 0.90$

Figure 14. Continued.

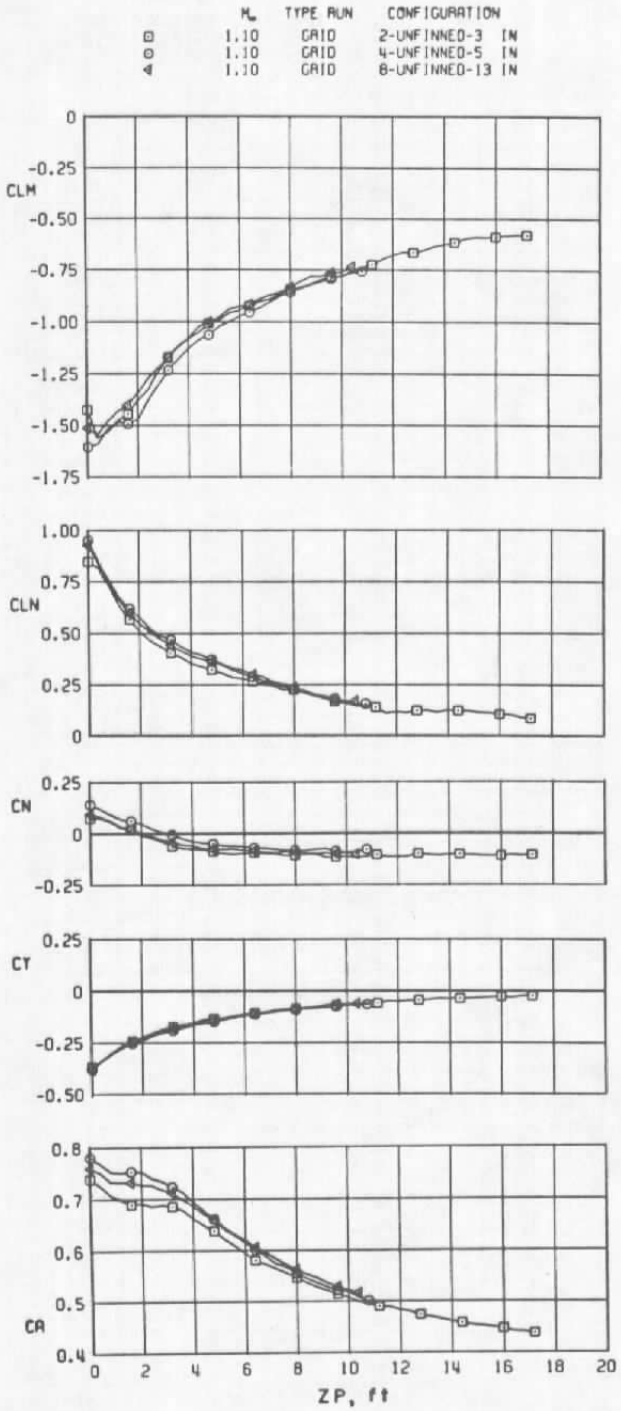


d. $M_\infty = 1.10$

**Figure 14. Continued.**

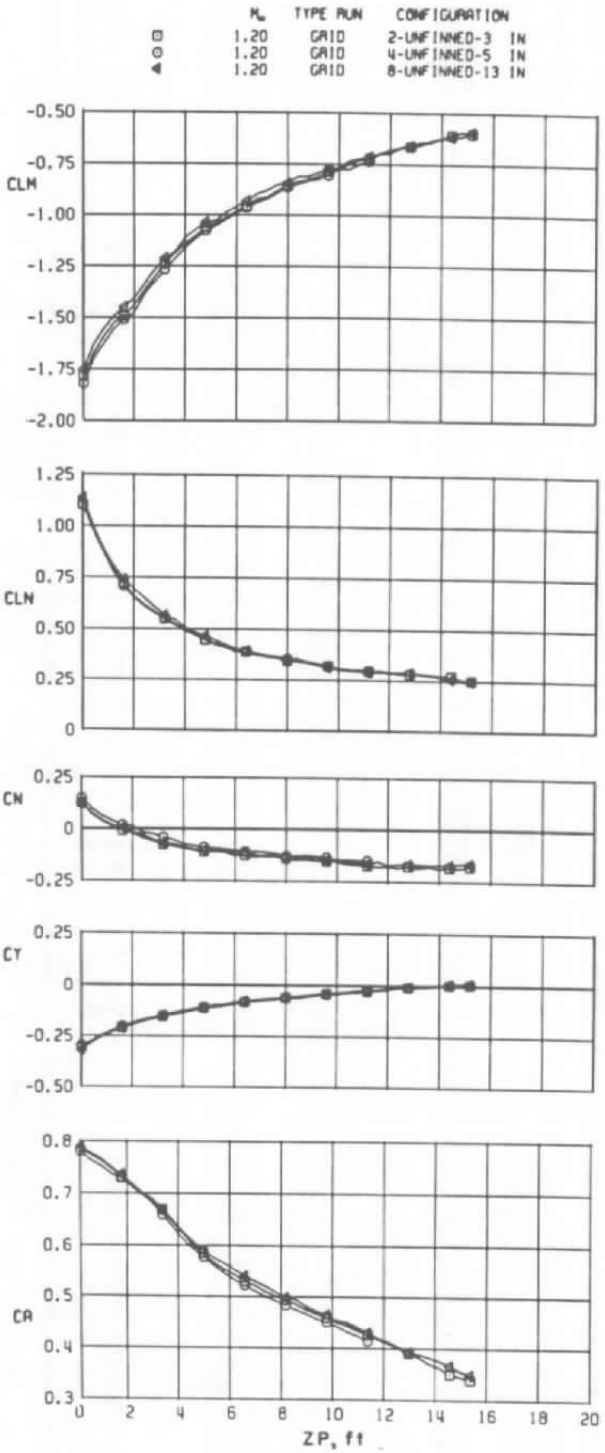


e. $M_\infty = 1.20$

Figure 14. Concluded.

**Table 1. Physical Characteristics of Both Stores (Assumed)**

| | |
|---|---|
| Model Reference Area | $S_m = 4.7274 \times 10^{-3}$ ft$^2$ |
| Model Span | $b_m = 9.3100 \times 10^{-1}$ in. |
| Model Moment Reference Length | $\bar{c}_m = 9.3100 \times 10^{-1}$ in. |
| Full-Scale Reference Area | $S' = 1.8910$ ft$^2$ |
| Full-Scale Span | $b' = 1.5517$ ft |
| Full-Scale Moment Reference Length | $\bar{c}' = 1.5517$ ft |
| Full-Scale Center-of-Gravity Location | $X_{cg} = 5.375$ ft (aft of nose) |
| Forward Ejector Force Location | $X_{L_1} = 0.8333$ ft forward of cg (full-scale) |
| Aft Ejector Force Location | $X_{L_2} = -0.8333$ ft aft of cg (full-scale) |
| Full-Scale Moment of Inertia (roll axis) | $I_{xx} = 12.0$ slug-ft$^2$ |
| Full-Scale Moment of Inertia (pitch axis) | $I_{yy} = 150$ slug-ft$^2$ |
| Full-Scale Moment of Inertia (yaw axis) | $I_{zz} = 150$ slug-ft$^2$ |
| Full-Scale Product of Inertia | $I_{xz} = 0$ slug-ft$^2$ |
| Full-Scale Store Weight | $W = 804$ lb |
| Flight Altitude of Full-Scale Vehicles | $h = 5{,}000$ ft |
| Pitch-Damping Coefficient (Assumed) | $C_{m_q} = -1{,}000$ per radian |
| Yaw-Damping Coefficient (Assumed) | $C_{n_r} = -1{,}000$ per radian |

## NOMENCLATURE

| | |
|---|---|
| $b_m$ | Store model fin span, in. |
| $b'$ | Full-scale fin span, ft |
| CA($C_A$) | Axial-force coefficient, $C_A = F_A/qS$ |
| CLM($C_m$) | Pitching-moment coefficient, $C_m = M_m/qS\bar{c}$ |
| CLN($C_n$) | Yawing-moment coeffient, $C_n = M_n/qS\bar{c}$ |
| $C_{m_q}$ | Pitch-damping coefficient, per radian |
| CN($C_N$) | Normal-force coefficient, $C_N = F_N/qS$ |
| $C_{n_r}$ | Yaw-damping coefficient, per radian |
| CY($C_y$) | Side-force coefficient, $C_y = F_y/qS$ |
| $\bar{c}_m$ | Model moment coefficient length, in. |
| $\bar{c}'$ | Full-scale moment coefficient length, ft |
| DPSI($\Delta\psi$) | Yaw angle (increment from carriage position), deg |
| DTHA($\Delta\theta$) | Pitch angle (increment from carriage position), deg |
| $F_A$ | Axial force, lb |
| $F_N$ | Normal force, lb |
| $F_y$ | Side force, lb |

| | |
|---|---|
| $h$ | Full-scale flight altitude, ft |
| $I_{xx}$ | Full-scale moment of inertia (roll axis), slug-ft$^2$ |
| $I_{xz}$ | Full-scale product of inertia, slug-ft$^2$ |
| $I_{yy}$ | Full-scale moment of inertia (pitch axis), slug-ft$^2$ |
| $I_{zz}$ | Full-scale moment of inertia (yaw axis), slug-ft$^2$ |
| $M_m$ | Pitching moment, in.-lb |
| $M_n$ | Yawing moment, in.-lb |
| $M_\infty$ | Free-stream Mach number |
| $P_t$ | Total pressure, psfa |
| $q_\infty$ | Free-stream dynamic pressure, lb/ft$^2$ |
| $S_m$ | Store model coefficient reference area, in.$^2$ |
| $S'$ | Full-scale store coefficient reference area, ft$^2$ |
| $UC_A$ | Uncertainty in axial-force coefficient |
| $UC_m$ | Uncertainty in pitching-moment coefficient |
| $UC_N$ | Uncertainty in normal-force coefficient |
| $UC_n$ | Uncertainty in yawing-moment coefficient |
| $UC_y$ | Uncertainty in side-force coefficient |

| | |
|---|---|
| $UM_\infty$ | Uncertainty in Mach number |
| $Uq_\infty$ | Uncertainty in free-stream dynamic pressure, $lb/ft^2$ |
| W | Full-scale store weight, lb |
| $X_{cg}$ | Full-scale store center of gravity, ft aft of nose |
| $X_{L_1}$ | Forward ejector force location, ft-forward of cg-full scale |
| $X_{L_2}$ | Aft ejector force location, ft-aft of cg-full scale |
| XP | Store axial position with respect to carriage position, ft-full scale |
| YP | Store lateral position with respect to carriage position, ft-full scale |
| ZP | Store vertical position with respect to carriage position, ft-full scale |